Article

Ruthenium(salen)-Catalyzed Aerobic Oxidative Desymmetrization of *meso*-Diols and Its Kinetics

Hideki Shimizu, Satoaki Onitsuka, Hiromichi Egami, and Tsutomu Katsuki

J. Am. Chem. Soc., **2005**, 127 (15), 5396-5413• DOI: 10.1021/ja047608i • Publication Date (Web): 23 March 2005

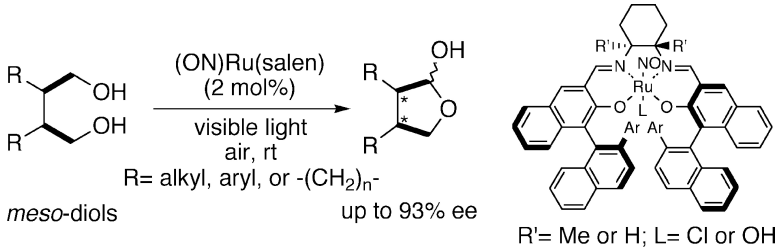

More About This Article

Additional resources and features associated with this article are available within the HTML version:

- Supporting Information
- Links to the 2 articles that cite this article, as of the time of this article download
- Access to high resolution figures
- Links to articles and content related to this article
- Copyright permission to reproduce figures and/or text from this article

View the Full Text HTML

J|A|C|S
ARTICLES
Published on Web 03/23/2005

Ruthenium(salen)-Catalyzed Aerobic Oxidative Desymmetrization of *meso*-Diols and Its Kinetics

Hideki Shimizu, Satoaki Onitsuka, Hiromichi Egami, and Tsutomu Katsuki*

Contribution from the Department of Chemistry, Faculty of Science, Graduate School, Kyushu University, CREST, Japan Science and Technology Agency (JST), Hakozaki, Higashi-ku, Fukuoka 812-8581, Japan

Received April 26, 2004; E-mail: katsuscc@mbox.nc.kyushu-u.ac.jp

Abstract: Chiral (nitrosyl)ruthenium(salen) complexes were found to be efficient catalysts for aerobic oxidative desymmetrization of *meso*-diols under photoirradiation to give optically active lactols. The scope of the applicability of this reaction ranges widely from acyclic diols to mono-cyclic diols, although fine ligand-tuning of the ruthenium(salen) complexes was required to attain high enantioselectivity (up to 93% ee). In particular, the nature of the apical ligand was found to affect not only enantioselectivity but also kinetics of the desymmetrization reaction. Spectroscopic analysis of the oxidation disclosed that irradiation of visible light is indispensable not only for dissociation of the nitrosyl ligand but also for single electron transfer from the alcohol-bound ruthenium ion to dioxygen.

1. Introduction

Asymmetric catalytic oxidative desymmetrization of *meso*-diols is a reaction of high synthetic use, because it can generate multiple asymmetric centers together with two different functional groups at a time. Especially when the substrate is a *meso*-primary diol, the product is an optically active lactol or lactone that is a useful chiral building block for organic synthesis. Thus, much effort has been directed toward this area of chemistry in both enzymatic[1] and chemical approaches.[2] Some oxidoreductases have been successfully used for this purpose.[3] For example, horse liver alcohol dehydrogenase has been reported to catalyze oxidative desymmetrization of *meso*-diols such as *cis*-1,2- or 1,3-bis(hydroxymethyl)cycloalkanes[3a−c,e] and acyclic 3-substituted-1,5-pentanediols[3d] to give the corresponding lactones with high, mostly complete enantioselectivities. In addition, oxidation of glycerol using galactose oxidase proceeds to give L-glyceraldehyde enantioselectively.[3g] Although enzymatic desymmetrization shows excellent enantioselectivity, its scope of application is rather limited to some specific substrates, as explained by the key-and-lock model. On the other hand, chemical approaches fall behind in terms of enantioselectivity, although several seminal studies have been reported for oxidative desymmetrization of prochiral and *meso*-diols. Electrooxidation of prochiral or *meso*-diols using a chirally modified electrode[4a] or chiral mediator[4b] is a promising approach: good to high enantioselectivity has been attained, albeit with limited prochiral substrates. Another interesting approach is asymmetric Oppenauer-type oxidation, an enantiotopos-selective hydrogen transfer reaction: chiral rhodium and ruthenium complexes have been used as catalyst for asymmetric desymmetrization, and moderate enantioselectivity has been realized.[5a−c] Recently, Hiroi et al. reported that enantioselectivity was improved up to 81% ee by using a chiral iridium catalyst, when some bicyclic *meso*-diols were used as substrates.[5d] It should be noted that products of these enzymatic and chemical oxidative desymmetrization reactions are lactones, which are produced by way of the corresponding lactols, except for the oxidation of glycerol, the product of which cannot make lactol.[3g] Various lactol subunits are, however, found in many natural products, and optically active lactols are useful synthetic intermediates. Therefore, exploitation of an efficient method for desymmetrization of *meso*-diols giving lactols without causing overoxidation to lactones has been strongly desired.

We have recently demonstrated that chiral (nitrosyl)ruthenium(salen) complexes [hereafter denoted as (ON)Ru(salen)s] are efficient catalysts for asymmetric aerobic oxidation reactions

(1) (a) Jones, J. B. In *Asymmetric Synthesis*; Morrison, J. D., Ed.; Academic Press: New York, 1984; Vol. 5, pp 309−344. (b) Faber, K. *Biotransformations in Organic Chemistry*, 3rd ed.; Springer: Berlin, 1997. (c) Bornscheuer, U. T.; Kazlauskas, R. J. *Hydrolases in Organic Synthesis*; Wiley−VCH: Weinheim, 1999. (d) Fantin, G.; Pedrini, P. In *Asymmetric Oxidation Reactions*; Katsuki, T., Ed.; Oxford University Press: Oxford, 2001; pp 200−214.

(2) For a review, see: Wills, M. C. *J. Chem. Soc., Perkin Trans. 1* **1999**, 1765−1784.

(3) (a) Jakovac, I. J.; Ng, G.; Lok, K. P.; Jones, J. B. *J. Chem. Soc., Chem. Commun.* **1980**, 515−516. (b) Jakovac, I. J.; Goodbrand, H. B.; Lok, K. P.; Jones, J. B. *J. Am. Chem. Soc.* **1982**, *104*, 4659−4665. (c) Lok, K. P.; Jakovac, I. J.; Jones, J. B. *J. Am. Chem. Soc.* **1985**, *107*, 2521−2526. (d) Irwin, A. J.; Jones, J. B. *J. Am. Chem. Soc.* **1977**, *99*, 556−561. (e) Bridges, A. J.; Raman, P. S.; Ng, G. S. Y.; Jones, J. B. *J. Am. Chem. Soc.* **1984**, *106*, 1461−1467. (f) Gais, H.-J.; Lukas, K. L.; Ball, W. A.; Braun, S.; Lindner, H. J. *Liebigs Ann. Chem.* **1986**, 687−716. (g) Klibanov, A. M.; Alberti, B. N.; Marletta, M. A. *Biophys. Res. Commun.* **1982**, *108*, 804−808.

(4) (a) Yanagisawa, Y.; Kashiwagi, Y.; Kurashima, F.; Anzai, J.-i.; Osa, T.; Bobbitt, J. M. *Chem. Lett.* **1996**, 1043−1044. (b) Tanaka, H.; Kawanami, Y.; Goto, K.; Kuroboshi, M. *Tetrahedron Lett.* **2001**, *42*, 445−448.

(5) (a) Ishii, Y.; Suzuki, K.; Ikariya, T.; Saburi, M.; Yoshikawa, S. *J. Org. Chem.* **1986**, *51*, 2822−2824. (b) Ishii, Y.; Osakada, K.; Ikariya, T.; Saburi, M.; Yoshikawa, S. *Chem. Lett.* **1982**, 1179−1182. (c) Asymmetric Oppenauer oxidation-like desymmetrization of *meso*-diols (up to 50% ee) has recently been reported: Ito, M.; Osaku, A.; Ikariya, T. The 81st Annual Meeting of the Chemical Society of Japan, Tokyo, March 2002; Abstr. No. 3 G4-14. (d) Suzuki, T.; Morita, K.; Matsuo, Y.; Hiroi, K. *Tetrahedron Lett.* **2003**, *44*, 2003−2006.

10.1021/ja047608i CCC: $30.25

Scheme 1

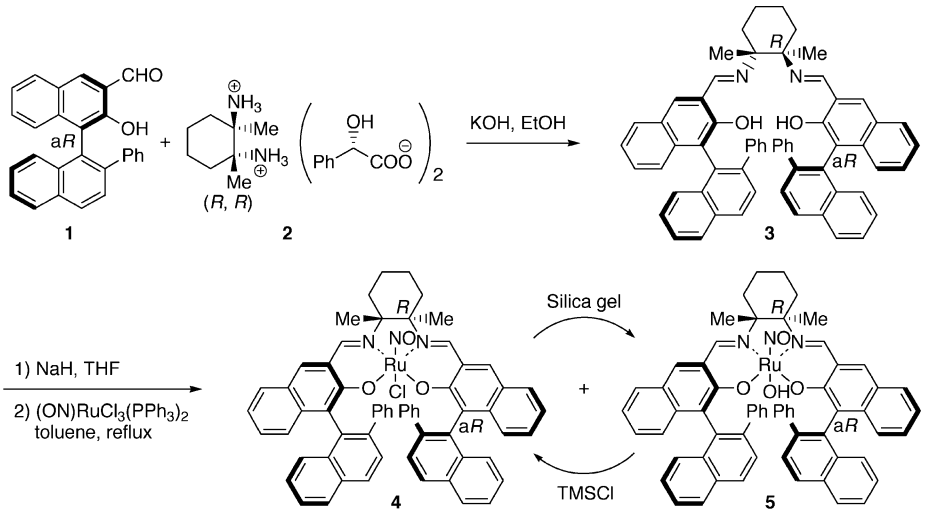

under photoirradiation: kinetic resolution of racemic secondary alcohols,[6a] oxidative coupling of β-naphthol,[6b] and oxidative cyclization of 2,2′-dihydroxy stilbene[6c] under irradiation of visible light.[7] In addition, we have disclosed that primary alcohols are selectively oxidized in the presence of secondary alcohols by using an achiral (ON)Ru(salen) bearing tetramethylethylenediamine as its diamine unit, as catalyst.[8a,9] Chemoselective aerobic oxidation of 1,*n*-diols giving the corresponding lactols has also been achieved by using the same (ON)Ru(salen).[8b] Lactol is usually equilibrated with the corresponding hydroxy aldehyde, but the equilibrium lists heavily to the lactol-side, when the ring size of the lactol is five or six. As lactol is a kind of secondary alcohol; no oxidation of the lactol is observed under the conditions. Of 1,ω-diols, therefore, 1,4- and 1,5-diols give the corresponding lactols exclusively when they are subjected to the above oxidation.[8b] Thus, we envisioned that desymmetrization of *meso*-1,4-diols giving optically active lactols would be realized by using a chiral (ON)Ru(salen) as the catalyst under aerobic and photoirradiated conditions.[10] After our paper on kinetic resolution,[6a] Sigman et al.[11a] and Stoltz et al.[11b] independently reported aerobic oxidative kinetic resolution using a palladium-sparteine system.[9e] Stoltz et al. also reported desymmetrization of σ-symmetric α,δ-secondary diols.[11b] In this paper, we describe in detail aerobic oxidative desymmetrization of *meso*-1,4-primary diols using various (ON)Ru(salen)s as catalysts.

2. Results and Discussion

2.1. Results of Desymmetrization of *meso*-Diols. Based on previous reports,[6,8] we first synthesized new (*R*,a*R*)-(ON)Ru(salen) complexes **4** and **5** bearing chiral quaternary carbons at the ethylenediamine unit (Scheme 1). The aldehyde **1**[12] and (1*R*,2*R*)-1,2-dimethyl-1,2-cyclohexanediammonium dimandelate (**2**)[13] prepared according to the reported procedures, respectively, were merely mixed in the presence of potassium hydroxide to give diimine **3** almost quantitatively. After diimine **3** was converted to its sodium salt, it was treated with $RuCl_3(NO)(PPh_3)_2$[14] in toluene under refluxing conditions to give a mixture of complex **4** bearing an apical chloro ligand and **5** bearing an apical hydroxo ligand. Fortunately, it was found that complex **4** could be converted into complex **5** by exposing it to acidic silica gel and **5** into **4** by treating it with chlorotrimethylsilane.[15] The corresponding (*S*,a*R*)-complex **8**, (*S*,a*S*)-(ON)Ru(salen) complexes (**9**, **10**, and **11**) bearing a bulkier 2-substituent (Ar) on the naphthalene ring at C3 and C3′ were also synthesized according to the same procedure (Figure 1).

With the complexes (**4**, **6**−**8**) bearing a chloro ligand at their apical position, we first examined aerobic oxidative desymmetrization of *cis*-1,2-bis(hydroxymethyl)cyclohexane (**12a**) in benzene at room temperature under photoirradiation (Table 1). Although **6** was an effective catalyst for kinetic resolution of racemic secondary alcohols,[6a] the desymmetrization with it was poorly enantioselective (entry 1). The reaction with **7** also showed marginal selectivity (entry 2). On the other hand, the enantioselectivity of the desymmetrization was considerably improved by using **4** or **8** as the catalyst (entries 3 and 4). In

(6) (a) Masutani, K.; Uchida, T.; Irie, R.; Katsuki, T. *Tetrahedron Lett.* **2000**, *41*, 5119−5123. (b) Irie, R.; Masutani, K.; Katsuki, T. *Synlett* **2000**, 1433−1436. (c) Masutani, K.; Irie, R.; Katsuki, T. *Chem. Lett.* **2002**, 36−37.
(7) (a) Katsuki, T. *Synlett* **2003**, 281−297. A detailed mechanism of photoactivation of (ON)Ru(salen)Cl complex has been reported: (b) Works, C. F.; Jocher, C. J.; Bart, G. D.; Bu, X.; Ford, P. C. *Inorg. Chem.* **2002**, *41*, 3728−3739. (c) Works, C. F.; Ford, P. C. *J. Am. Chem. Soc.* **2000**, *122*, 7592−7593. (d) Bordini, J.; Hughes, D. L.; Da Motta Neto, J. D.; da Cunha, C. J. *Inorg. Chem.* **2002**, *41*, 5410−5416.
(8) (a) Miyata, A.; Murakami, M.; Irie, R.; Katsuki, T. *Tetrahedron Lett.* **2001**, *42*, 7067−7070. (b) Miyata, A.; Furukawa, M.; Irie, R.; Katsuki, T. *Tetrahedron Lett.* **2002**, *43*, 3481−3484.
(9) For the review of aerobic oxidation of alcohols, see: (a) Sheldon, R. A.; Arends, I. W. C. E. In *Advances in Catalytic Activation of Dioxygen by Metal Complexes*; Simandi, L. I., Ed.; Kluwer Academic Publishers: Dordrecht, 2003; pp 123−155. (b) Sigman, M. S.; Jensen, D. R.; Rajaram, S. *Curr. Opin. Drug Discovery Dev.* **2002**, *5*, 860−869. (c) Marcó, I. E.; Giles, P. R.; Tsukazaki, M.; Brown, S. M.; Urch, C. J. In *Transition Metals for Organic Synthesis*; Beller, M., Bolm, C., Eds.; Wiley−VCH: Weinheim, 1999; Vol. 2, pp 350−360. (d) Nishimura, T.; Uemura, S. *Synlett* **2004**, 201−216. (e) Stoltz, B. M. *Chem. Lett.* **2004**, *33*, 362−367.
(10) A part of this study has been communicated: (a) Shimizu, H.; Nakata, K.; Katsuki, T. *Chem. Lett.* **2002**, 1080−1081. (b) Shimizu, H.; Katsuki, T. *Chem. Lett.* **2003**, 480−481.
(11) (a) Jensen, D. R.; Pugsley, J. S.; Sigman, M. S. *J. Am. Chem. Soc.* **2001**, *123*, 7475−7476. (b) Ferreira, E. M.; Stoltz, B. M. *J. Am. Chem. Soc.* **2001**, *123*, 7725−7726.
(12) Sasaki, H.; Irie, R.; Hamada, T.; Suzuki, K.; Katsuki, T. *Tetrahedron* **1994**, *50*, 11827−11838.
(13) Zhang, W.; Jacobsen, E. N. *Tetrahedron Lett.* **1991**, *32*, 1711−1714.
(14) Levison, J. J.; Robinson, S. D. *J. Chem. Soc. A* **1970**, 96−99.
(15) Complex **4** was completely converted into complex **5**, when it was exposed to silica gel (FL100B, Fuji Silysia Chemical Ltd.) in CH_2Cl_2 for 12 h. On the other hand, treatment of **5** with chlorotrimethylsirane in CH_2Cl_2 gave **4**. Complexes **5** and **4** were isolated in moderate yields (50−70%) after purification by silica gel chromatography. IR spectra of **5** showed the absorption at 3540 cm^{-1} characteristic of the OH group, while those of **4** did not show such absorption.

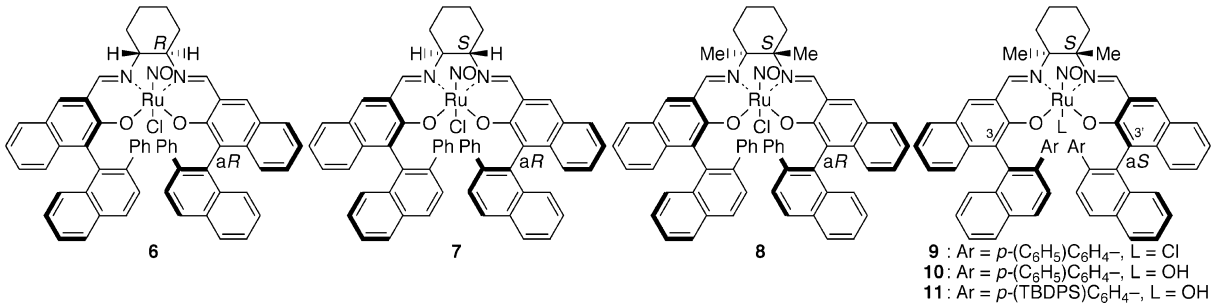

Figure 1.

Table 1. Desymmetrization of *cis*-1,2-Bis(hydroxymethyl)cycloalkanes **12** Using Various (ON)Ru(salen)s as Catalyst[a]

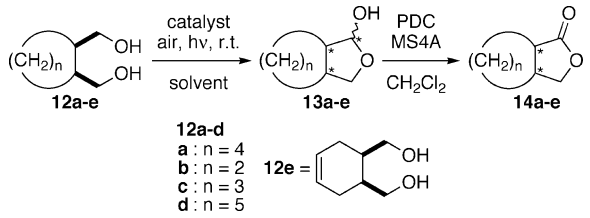

entry	catalyst	substrate	solvent	time/d	yield/%[b]	% ee[c]	config.[d]
1	**6**	**12a**	benzene	0.75	81	4	1*S*, 6*R*
2	**7**	**12a**	benzene	0.75	73	7	1*R*, 6*S*
3	**4**	**12a**	benzene	0.75	53	55	1*S*, 6*R*
4	**8**	**12a**	benzene	0.75	11	22	1*R*, 6*S*
5	**4**	**12a**	toluene	1	29	53	1*S*, 6*R*
6	**4**	**12a**	AcOEt	1	77	58	1*S*, 6*R*
7	**4**	**12a**	THF	1	21	52	1*S*, 6*R*
8	**4**	**12a**	acetone	1	16	51	1*S*, 6*R*
9	**4**	**12a**	PhCl	1	33	55	1*S*, 6*R*
10	**4**	**12a**	CH_2Cl_2	1	35	65	1*S*, 6*R*
11	**4**	**12a**	$CHCl_3$	1	54	67	1*S*, 6*R*
12	**5**	**12a**	$CHCl_3$	2.5	28	70	1*S*, 6*R*
13	**9**	**12a**	$CHCl_3$	2.5	23	71	1*R*, 6*S*
14	**10**	**12a**	$CHCl_3$	2.5	14	81	1*R*, 6*S*
15	**11**	**12a**	$CHCl_3$	2.5	20	59	1*R*, 6*S*
16[e]	**10**	**12a**	$CHCl_3$	7	80	80	1*R*, 6*S*
17[e]	**10**	**12b**	$CHCl_3$	7	64	74	1*S*, 5*R*
18[e]	**10**	**12c**	$CHCl_3$	7	78	66	1*S*, 5*R*
19[e]	**10**	**12d**	$CHCl_3$	7	80	63	[f]
20[e]	**10**	**12e**	$CHCl_3$	7	68	75	1*R*, 6*S*[g]

[a] Reactions were carried out at room temperature in air under irradiation using a halogen lamp as the light source. [b] Isolated yield of lactol. [c] Determined by GLC analysis using optically active column (SUPELCO BETA-DEX-225) after its conversion to the corresponding lactones. [d] Determined by comparison of the specific rotation after its conversion to the corresponding lactones [ref 3b], unless otherwise mentioned. For the number locant of each product, see the Experimental Section. [e] 4 mol % of the catalyst was used. [f] The absolute configuration has not been determined. [g] Reference 3f.

particular, the desymmetrization with **4** showed remarkably improved enantioselectivity of 55% ee (entry 3). These results indicated that the presence of the two chiral groups, a chiral quaternary carbon at the ethylenediamine unit and the axially chiral binaphthyl group, is essential for achieving enantiotopos selection in the present desymmetrization, and the (*R*)-quaternary carbon and the (a*R*)-binaphthyl group are a synergistic combination for better asymmetric induction.

We next examined the effect of the solvent on enantioselectivity by using **4** as the catalyst (entries 5−11). Although the solvent effect was small, the reactions in halocarbons showed somewhat improved enantioselectivity (entries 10 and 11), and the best enantioselectivity was observed when the reaction was carried out in chloroform.

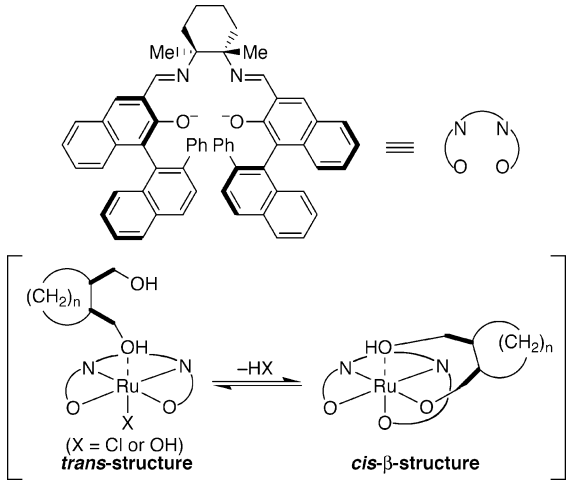

Figure 2.

Salen complexes of second low transition metals tend to adopt the *cis*-β configuration,[16,17] and the hydroxo ligand bound to the transition metal in general undergoes alkoxide ligand exchange smoothly. Thus, the desymmetrization of **12a** was further examined in chloroform with complex **5** bearing an apical hydroxo (X = OH) ligand as the catalyst, with the expectation that the diol would make a chelate with the ruthenium ion and enantioselectivity of the reaction would be improved (Figure 2). As expected, enantioselectivity was enhanced, albeit slightly, to 70% ee (entry 12).[18] Encouraged by these results, we further attempted adjusting the 2-substituent of the naphthyl group at C3 and C3′ in anticipation that the 2-substituent would exert a strong influence on asymmetric induction. Thus, we examined the reaction with complexes **9**, **10**, and **11** (entries 13−15). Although use of **11** as the catalyst reduced enantioselectivity, use of **10** improved enantioselectivity up to 81% ee. It is noteworthy that the complexes (**10** and **5**) bearing a hydroxo ligand exhibit higher enantioselectivity than the complexes (**9** and **4**) bearing a chloro ligand, respectively, but the former complexes are inferior to the latter in catalytic reactivity (entries 11−14). With these results, we examined the desymmetrization of several other monocyclic 1,4-*meso*-diols **12a**−**e** by using 4 mol % of **10** as catalyst (entries 16−20). The reactions showed moderate to good enantioselectivity under ambient conditions.

(16) (a) Sauve, A. A.; Groves, J. T. *J. Am. Chem. Soc.* **2002**, *124*, 4770−4778. (b) Corazza, F.; Solari, E.; Floriani, C.; Chiesi-Villa, A.; Guastini, C. *J. Chem. Soc., Dalton Trans.* **1990**, 1335−1344.
(17) Watanabe, A.; Uchida, T.; Irie, R.; Katsuki, T. *Proc. Natl. Acad. Sci. U.S.A.* **2004**, *101*, 5737−5742.
(18) This working hypothesis was found to be inconsistent with the kinetic study: see the section for kinetic study.

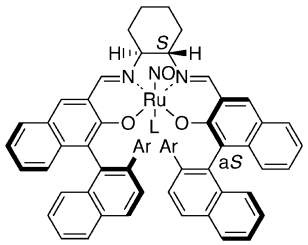

17 : Ar = *p*-(TBDPS)C_6H_4–, L = Cl
18 : Ar = *p*-(TBDPS)C_6H_4–, L = OH

Figure 3.

Table 2. Desymmetrization of 2,3-Diphenylbutane-1,4-diol (**15**)[a]

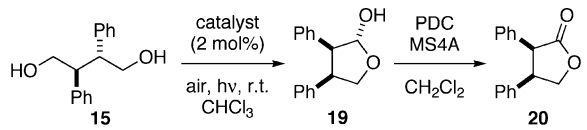

15 **19** **20**

entry	catalyst	yield/%[b]	% ee[c,d]
1	**4**	82	81
2	**5**	87	77
3	**6**	62	50
4	**10**	55	79
5	**11**	68	52
6	**17**	67	68

[a] Reactions were carried out under irradiation using a halogen lamp as the light source. [b] Isolated yield of lactol. [c] Determined by HPLC using DAICEL CHIRALCEL OD-H (*n*-hexane/*i*-PrOH = 9/1, flow rate 0.7 mL/min) after conversion to the corresponding lactone **20**. [d] The absolute configuration has not been determined.

Up to this time, we attempted optimization of this oxidation by using *meso*-diol **12a** as the test material. To clarify the scope of this reaction, we further examined desymmetrization of acyclic and bulky cyclic *meso*-1,4-diols. Thus, we next examined desymmetrization of acyclic *meso*-2,3-disubstituted butane-1,4-diols (**15** and **16**) using various (ON)Ru(salen) complexes (Figures 1 and 3), and complex **4** bearing a chloro ligand was found to be the catalyst of choice for the desymmetrization of *meso*-2,3-diphenylbutane-1,4-diol (**15**) (81% ee, 82% yield, Table 2, entry 1). Complex **5** was slightly inferior to complex **4** (entry 2). Complex **10** bearing a 2-(4-biphenylyl)naphthyl group at C3 and C3′ and an apical hydroxo ligand also showed somewhat inferior enantioselectivity (79% ee, entry 4). To our surprise, complex **17** that has no chiral quaternary carbons at its diamine unit but possesses a bulky group at C3 and C3′ showed moderate enantioselectivity (68% ee, entry 6).

On the other hand, desymmetrization of *meso*-2,3-dicyclohexylbutane-1,4-diol (**16**) was poorly effected by either **4**, **6**, or **10** bearing a relatively small phenyl or 4-biphenyly group as 2-substituent (Table 3, entries 1−3). However, complex **11** bearing a bulky 2-[*p*-(*tert*-butyldiphenysilyl)phenyl]naphthyl group at C3 and C3′ showed moderate enantioselectivity of 61% ee, although the chemical yield of the lactol was badly diminished due to the formation of unidentified products (entry 4).[19] Fortunately, the reaction with complex **17** lacking the quaternary chiral carbons showed moderate, but the best, enantioselectivity (entry 5). The product did not include lactone, the overoxidized product.

Desymmetrization of bulky cyclic *meso*-diols, *cis*-1,2-bis(hydroxymethyl)-3,6-diphenylcyclohexane (**23a**) and *cis*-1,2-bis-

(19) ^{1}H NMR (400 MHz) analysis of the products indicated the formation of the acetals from the resulting aldehyde and the starting diol.

Table 3. Desymmetrization of 2,3-Dicyclohexylbutane-1,4-diol (**16**)[a]

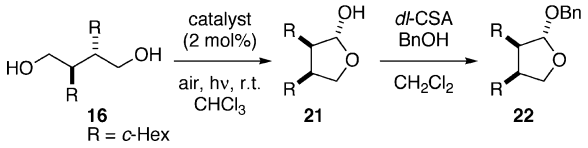

16 R = *c*-Hex **21** **22**

entry	catalyst	time/d	yield/%[b]	% ee[c−e]
1	**4**	3	40	9
2	**6**	3	90	9
3	**10**	2.5	68	1
4	**11**	1.5	10	61
5	**17**	4	82	62
6	**18**	3.5	72	54

[a] Reactions were carried out under irradiation using a halogen lamp as the light source. [b] Isolated yield of lactol that included a single anomeric isomer. The configuration of the anomeric carbon was determined to be trans by NOE study. [c] Determined by HPLC analysis using DAICEL CHIRALPAK AD-H (*n*-hexane/*i*-PrOH = 99.9/0.1, flow rate 0.16 mL/min) after its conversion to the corresponding benzyl acetals. [d] When the lactol **21** was converted to benzyl acetal (**22**), a small amount of the corresponding β-isomer was also formed. Enantiomeric excesses of α- and β-isomers were identical. [e] Absolute configuration has not been determined.

Table 4. Desymmetrization of 3,6-Disubstituted *meso*-Diols **23a**,**b**[a]

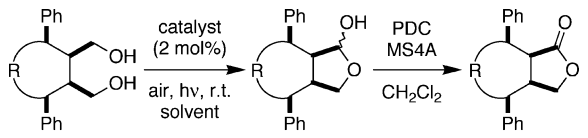

23a : R = –CH_2–CH_2–
23b : R = –CH=CH–
24a,b **25a,b**

entry	substrate	catalyst	time/d	yield/%[b]	% ee[c]
1	**23a**	**4**	7	90	16
2	**23a**	**5**	7	44	31
3	**23a**	**10**	7	52	36
4	**23a**	**11**	7	39	81
5	**23a**	**17**	3	77	93
6	**23a**	**18**	7	58	83
7[d]	**23a**	**17**	2	99	93
8[d]	**23a**	**18**	3	98	81
9	**23b**	**4**	7	73	21
10	**23b**	**5**	7	70	39
11	**23b**	**11**	5	84	76
12	**23b**	**17**	4	82	90
13[d]	**23b**	**17**	2	96	90
14[d]	**23b**	**18**	5	99	81

[a] Reactions were carried out under irradiation using a halogen lamp as the light source. [b] Isolated yield of lactol. [c] Determined by HPLC using DAICEL CHIRALCEL OD-H (*n*-hexane/*i*-PrOH = 4/1, flow rate 0.7 mL/min) after its conversion to the corresponding lactone. [d] 4 mol % of the catalyst was used.

(hydroxymethyl)-3,6-diphenylcyclohex-4-ene (**23b**), was also examined (Table 4). None of complexes **4**, **5**, and **10** that were efficient for desymmetrization of *meso*-diols so far examined were very useful for desymmetrization of the *meso*-diol **23a** (entries 1−3). Again, complex **11** bearing the bulky C2-group showed remarkably enhanced enantioselectivity of 81% ee, albeit with moderate chemical yield (entry 4). Use of complex **17** bearing cyclohexanediamine as the diamine unit further improved enantioselectivity (up to 93% ee) and chemical yield (entry 5). The lactol was obtained in almost quantitative yield without diminishing enantioselectivity when 4 mol % of complex **17** was used (entry 7). The corresponding hydroxo complex **18** was slightly less efficient (entries 6 and 8). Desymmetrization of **23b** was also successfully effected by using **17** as catalyst (90% ee, 96% yield, entry 13). For this

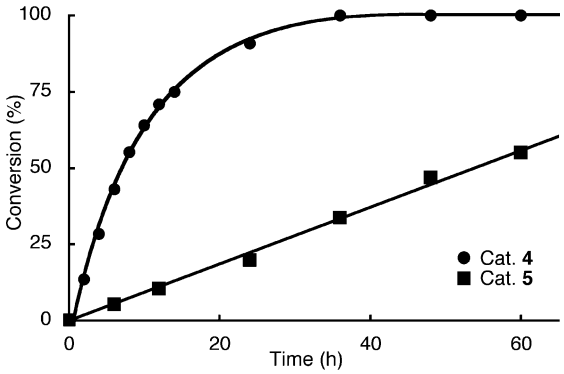

Figure 4. Oxidation of **12a** with complex **4** or **5** as catalyst. Conditions: 2 mol % of catalyst, diol **12a** in benzene-d_6 (0.1 M, 1 mL), under irradiation in air at ambient temperature.

Scheme 2

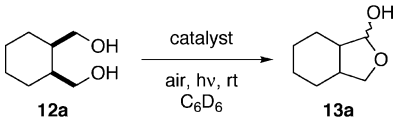

oxidation, complex **18** was also slightly less efficient than complex **17** (entry 14).

With these results, we examined oxidation of **12a** using **17** or **18** as catalyst, but the enantioselectivities observed were moderate (33 and 38% ee's, respectively).

As described above, the best catalyst for the present desymmetrization was found to vary with the substrate used: the desymmetrization of less bulky *meso*-cyclic diols (**12**) was best effected by complex **10** bearing an apical hydroxo ligand, while that of acyclic (**15** and **16**) and bulky cyclic *meso*-diols (**23**) was better effected by the catalysts bearing an apical chloro ligand such as **4** and **17** than by the catalysts bearing an apical hydroxo ligand such as **5** and **18**. These results suggested that the mechanism of molecular recognition by a complex bearing an apical chloro ligand is different from that by a complex bearing an apical hydroxo ligand. To shed light on the mechanism of the present aerobic oxidative desymmetrization, we carried out the following mechanistic studies.

2.2. Mechanistic Studies on Desymmetrization. Kinetic Studies during Catalytic Turnover. At first, we carried out several kinetic studies using *cis*-1,2-bis(hydroxymethyl)cyclohexane (**12a**) as the test material and complexes **4** and **5** as catalysts to understand the difference in the catalysis between the complexes bearing an apical chloro ligand and the complexes bearing an apical hydroxo ligand (Scheme 2). These studies disclosed several interesting phenomena of the present oxidation. The plot of conversion of the starting material versus reaction time indicated that the rate of the oxidation using **5** did not depend on the substrate concentration but on the catalyst concentration (Figures 4 and 5), while the rate of the oxidation using **4** depended on both the catalyst and the substrate concentrations (Figures 4 and 6). In accord with this, the reaction rate with complex **5** was in proportion to catalyst loading: the slope of the plot (conversion of the starting material vs reaction time) showed a linear correlation with the catalyst loading (Figure 5). The plot of $-\ln[S]/[S_0]$ versus reaction time indicated that the reaction with **4** was first-order in substrate concentration and the slope of the $-\ln[S]/[S_0]$ versus the reaction time showed a linear correlation with the catalyst loading, indicating that the oxidation rate was also in proportion to catalyst loading (Figure 6). The experimental data obtained within ca. 10% conversion were used for these and the following discussions. It is also noteworthy that the initial relative conversion rate of **12a** in the reactions with **4** and **5** was calculated to be ca. 16 from the slopes of the plots of conversion versus reaction time (Figure 4).

We next examined the dependence of the oxidation rates on dioxygen concentration by using a recently published technique,[20] and the plots of log k versus log $[O_2]$ disclosed that the rate of the oxidation with **4** showed first-order dependence on dioxygen concentration, while the order of the oxidation with **5** in terms of dioxygen was determined to be 0.42 (Figure 7). Thus, the rate laws for the oxidation of **12a** with **4** and **5** are rate $= k_1$[**12a**][**4**][O_2] and rate $= k_2$[**5**][O_2]$^{0.42}$, respectively.

To know whether the above unique mechanism is limited to the oxidation of diols or not, we also carried out kinetic studies on the oxidation of a simple mono-ol, 3-phenylpropanol (**26**), as substrate. As shown in Figure 8, the kinetics observed in these reactions are very similar to those observed in the oxidation of **12a**: the rate of the oxidation with **4** depends on both the substrate and the catalyst concentrations, while the oxidation with **5** depends only on catalyst concentration. Again, the oxidation with **4** showed a ca. first-order dependence (order $= 1.12$) on dioxygen concentration, while the order of the oxidation with **5** in terms of dioxygen was determined to be 0.33. Thus, the rate laws for the oxidation of **26** with **4** and **5** are rate $= k_3$[**26**][**4**][O_2] and rate $= k_4$[**5**][O_2]$^{0.33}$, respectively.

Although we assumed that the oxidation of **12a** with **5** bearing an apical hydroxo ligand might proceed via a chelate intermedi-

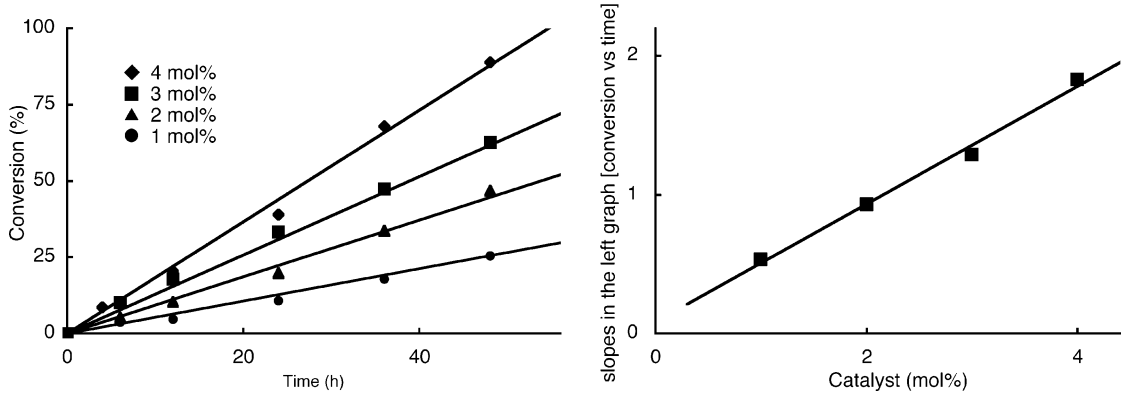

Figure 5. Correlation between reaction rate and catalyst loading in the oxidation with **5**. Conditions: diol **12a** in benzene-d_6 (0.1 M, 1 mL), under irradiation in air at ambient temperature. The range of the loading of **5** is 1−4 mol %.

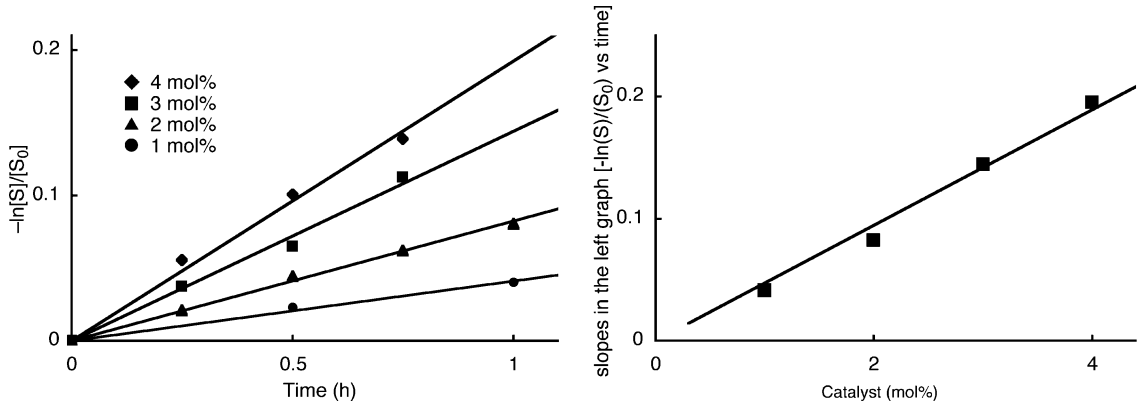

Figure 6. Correlation between reaction rate and catalyst loading in the oxidation with **4**. Conditions: diol **12a** in benzene-d_6 (0.1 M, 1 mL), under irradiation in air at ambient temperature. The range of the loading of **4** is 1−4 mol %.

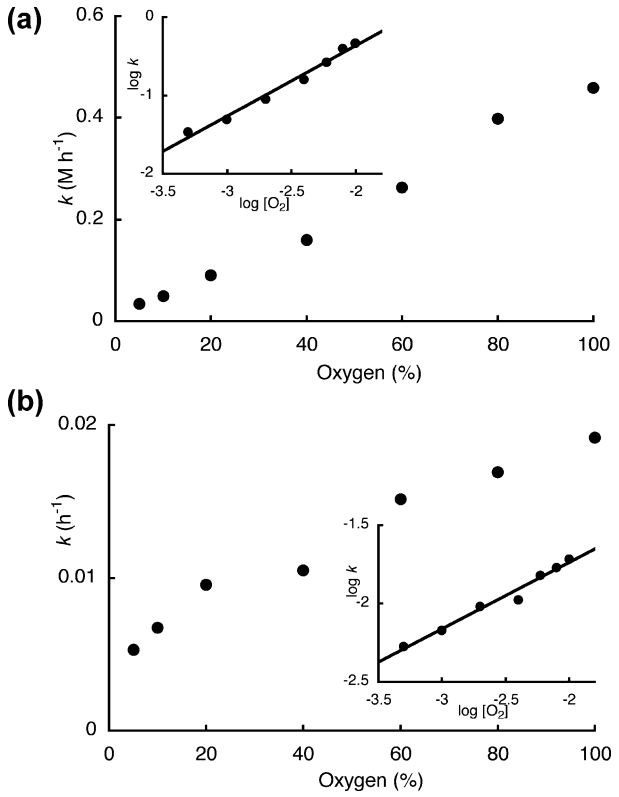

Figure 7. (a) Plot of the reaction rate with **4** versus dioxygen concentration. Conditions: 2 mol % of **4**, diol **12a** in benzene-d_6 (0.1 M, 1 mL), under irradiation in air at ambient temperature, with a balloon charged with N_2/O_2 mixture. The range of oxygen concentration is 5−100%. Inset: log k versus log[O_2]. (b) Plot of reaction rate with **5** versus dioxygen concentration. Conditions: 2 mol % of **5**, diol **12a** in benzene-d_6 (0.1 M, 1 mL), under irradiation in air at ambient temperature, with a balloon charged with N_2/O_2 mixture. The range of oxygen concentration is 5−100%. Inset: log k versus log[O_2].

ate (Figure 2), the fact that the kinetics for the oxidation of mono-ol **26** closely resemble that of diol **12a** (Figures 4 and 8) does not seem to support this assumption.

Kinetic Isotope Effect. Two reaction mechanisms, one including a tandem SET and hydrogen atom transfer process[21] and the other including a β-hydrogen elimination process,[20,22,23] have been proposed for metal-catalyzed oxidation of alcohols, and ruthenium- and palladium-catalyzed oxidations of alcohols have been mostly proposed to proceed via a β-hydrogen elimination process.[9d,e,20,24,25]

To get more information about the mechanism of the present oxidation, we next measured the kinetic isotope effect (KIE) of the present reactions using **12a** and **26** as substrates (Scheme 3). The observed H/D relative reaction rate (k_H/k_D) of **12a** and **12a**-d_4 with **4** as the catalyst was 1.34 (Table 5, entry 1).[26] A similar level of small k_H/k_D (1.55) was observed in the reaction with **5** as the catalyst (entry 2). These k_H/k_D values were determined by independent measurement of the reaction rates with **12a** and **12a**-d_4 as the substrates. KIE for the oxidation of **26** was studied with **26**, racemic **26**-α-d_1, and **26**-α,α-d_2 (entries 3−8): Intramolecular KIEs (KIE_{intra}) measured with **26**-α-d_1 as the substrate (intramolecular competition) were determined to be 6.18 and 5.23 for the oxidation with **4** and **5**, respectively (entries 5 and 6), while intermolecular KIEs (KIE_{inter}) measured by the oxidation of a mixture of **26** and **26**-α,α-d_2 with **4** or **5** (intermolecular competition) were determined to be 10.7 and 3.42, respectively (entries 7 and 8).[27] On the other hand, $KIEs_{inter}$ determined by independent measurement of the reaction rates with **26** and **26**-α,α-d_2 as the substrates were 1.40 and 2.51 for the oxidation with **4** and **5**, respectively (entries 3 and 4).

The magnitude of KIE in oxidation of alcohols varies with the reaction mechanism, the substrate used, and the method of measurement. The k_H/k_D values for oxidation with galactose oxidase or its model compounds,[28−30] a Cu(II)-Schiff base catalyst,[31] and a Cu(I)-TEMPO system,[32] which has been proposed to proceed via hydrogen atom transfer from the

(20) Mueller, J. A.; Goller, C. P.; Sigman, M. S. *J. Am. Chem. Soc*. **2004**, *126*, 9724−9734.
(21) (a) Kirihara, M.; Ichinose, M.; Takizawa, S.; Momose, T. *Chem. Commun.* **1998**, 1691−1692. (b) Morrison, V.; Barnier, J.-P.; Blanco, L. *Tetrahedron Lett*. **1999**, *40*, 4045−4046. (c) Kulincovich, O. G.; Astashko, D. A.; Tyvorskii, V. I.; Ilina, N. A.; *Synthesis* **2001**, 1453−1455.
(22) (a) Noyori, R.; Yamakawa, M.; Hashiguchi,S. *J. Org. Chem.* **2001**, *66*, 7931−7944. (b) Nishibayashi, Y.; Yamauchi, A.; Onodera, G.; Uemura, S. *J. Org. Chem.* **2001**, *68*, 5875−5880. (c) Pamies, O.; Backvall, J. E. *Chem.-Eur. J.* **2001**, *7*, 5052−5058. (d) Dijksman, A.; Marino-Gonzalez, A.; Payeras, A. M. I.; Arends, I. W. C. E.; Sheldon, R. A. *J. Am. Chem. Soc.* **2001**, *123*, 6826−6833. (e) Sharpless, K. B.; Akashi, K.; Oshima, K. *Tetrahedron Lett.* **1976**, *17*, 2503−2506.
(23) Kulinkovich, O. G. *Chem. Rev.* **2003**, *103*, 2597−2632.
(24) Yamaguchi, K.; Mizuno, N. *Angew. Chem., Int. Ed.* **2002**, *41*, 4538−4541.
(25) Naota, T.; Takaya, H.; Murahashi, S.-I. *Chem. Rev.* **1988**, *88*, 2599−2660.
(26) The kinetic experimental protocol is given in the Experimental Section.
(27) This experiment was carried out according to the kind suggestions of a reviewer, to whom we are very grateful.
(28) Minasian, S. G.; Whittaker, M. M.; Whittaker, J. W. *Biochemistry* **2004**, *43*, 13683−13693.
(29) Pratt, R. C.; Stack, T. D. P. *J. Am. Chem. Soc.* **2003**, *125*, 8716−8717.
(30) Whittaker, M. M.; Whittaker, J. W. *Biochemistry* **2001**, *40*, 7140−7148.
(31) Wang, Y.; DuBois, J. L.; Hedman, B.; Hodgson, K. O.; Stack, T. D. P. *Science* **1998**, *279*, 537−540.
(32) Dijksman, A.; Arends, I. W. C. E.; Sheldon, R. A. *Org. Biomol. Chem.* **2003**, *1*, 3232−3237.

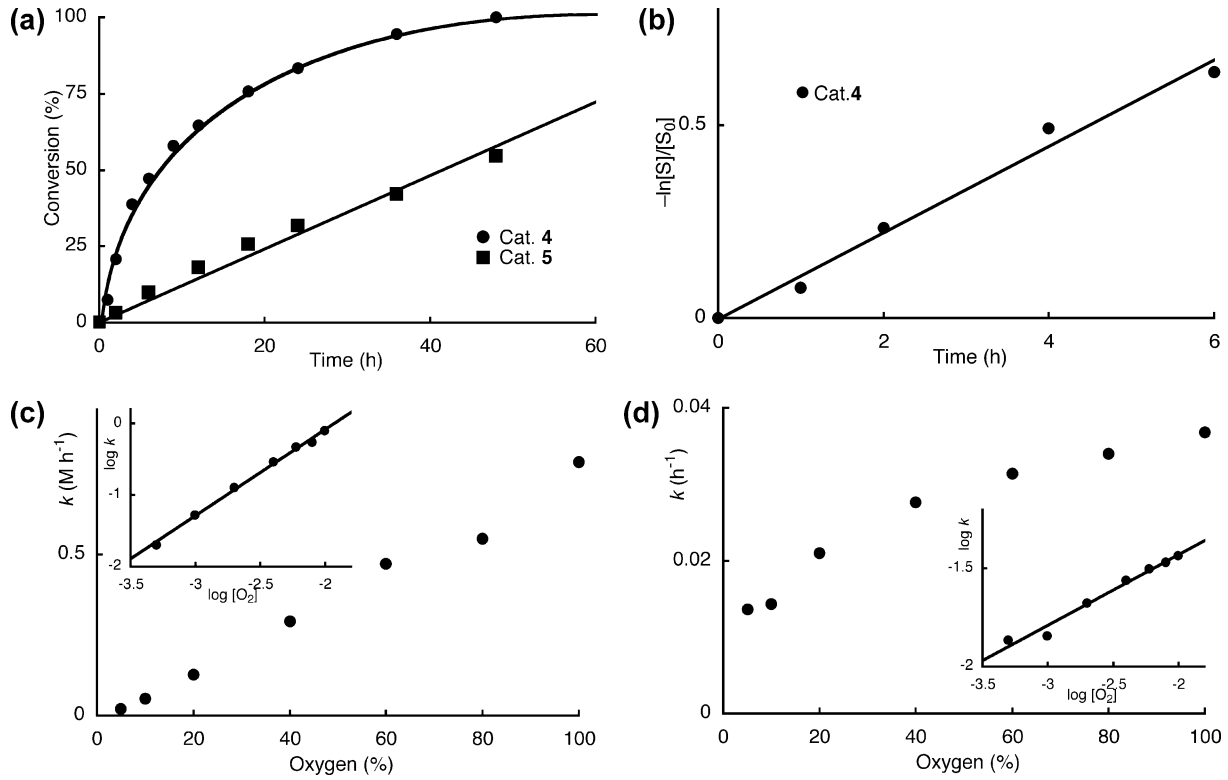

Figure 8. (a) Oxidation of **26** with complex **4** or **5** as catalyst. Conditions: 2 mol % of catalyst, alcohol **26** in benzene-d_6 (0.1 M, 1 mL), under irradiation in air at ambient temperature. (b) Relationship between $-\ln[\mathbf{26}]/[\mathbf{26}_0]$ versus reaction time. Conditions: as described in (a). (c) Plot of the reaction rate with **4** versus dioxygen concentration. Conditions: 2 mol % of **4**, alcohol **26** in benzene-d_6 (0.1 M, 1 mL), under irradiation in air at ambient temperature, with a balloon charged with N_2/O_2 mixture. The range of oxygen concentration is 5−100%. Inset: log k versus log[O_2]. (d) Plot of the reaction rate with **5** versus dioxygen concentration. Conditions: 2 mol % of **5**, alcohol **26** in benzene-d_6 (0.1 M, 1 mL), under irradiation in air at ambient temperature, with a balloon charged with N_2/O_2 mixture. The range of oxygen concentration is 5−100%. Inset: log k versus log[O_2].

Scheme 3

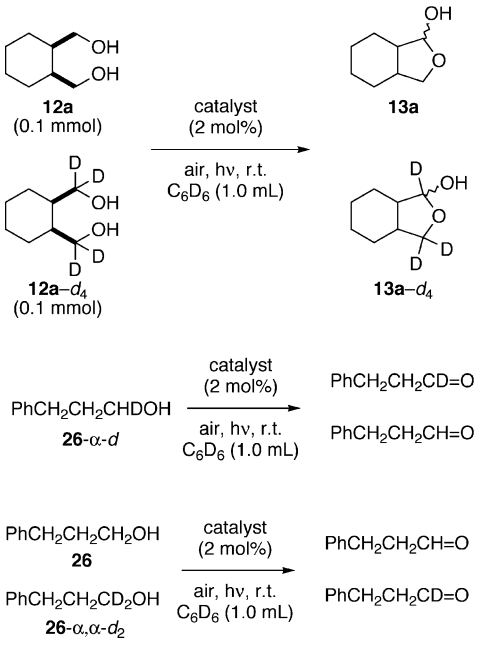

corresponding metal alkoxides, range from 3 to 7. On the other hand, oxidation of alcohols using potent one-electron oxidants such as cerium(IV) sulfate and manganese(III) sulfate has been reported to show small KIE values ($k_H/k_D = 1.6-1.9$),[33,34] which indicates that generation of an oxygen radical facilitates hydrogen atom abstraction next to the radical and a small k_H/k_D value is observed for such hydrogen atom abstraction. Thus, the k_H/k_D values observed in the oxidation of **26** under intermolecular competitive condition are adequate for the KIE of hydrogen atom transfer from a ruthenium alkoxide. KIE for hydrogen atom transfer is associated with two factors: primary KIE arising from the isotopic substitution of the atom at the

Table 5. Kinetic Isotope Effects Observed in the Ru(salen)-Catalyzed Aerobic Oxidation of Several Alcohols[a]

Independent Measurement

entry	substrate	catalyst	KIE (k_H/k_D)[b]
1	**12a**/**12a**-d_4	**4**	1.34 ± 0.04
2	**12a**/**12a**-d_4	**5**	1.55 ± 0.02
3	$Ph(CH_2)_3OH/Ph(CH_2)_2CD_2OH$	**4**	1.40 ± 0.03
4	$Ph(CH_2)_3OH/Ph(CH_2)_2CD_2OH$	**5**	2.51 ± 0.05

Intra- or Intermolecular Competition

entry	substrate	catalyst	KIE (H/D)[b]
5	$Ph(CH_2)_2CHDOH$	**4**	6.18 ± 0.04
6	$Ph(CH_2)_2CHDOH$	**5**	5.23 ± 0.02
7	$Ph(CH_2)_3OH/Ph(CH_2)_2CD_2OH$	**4**	10.7 ± 0.2
8	$Ph(CH_2)_3OH/Ph(CH_2)_2CD_2OH$	**5**	3.42 ± 0.09

[a] Reactions were carried out under standard conditions. [b] H/D ratios were determined by ^1H NMR analysis. The KIE value is an average of three runs.

(33) (a) Littler, J. S. *J. Chem. Soc.* **1959**, 4135−4136. (b) Littler, J. S. *J. Chem. Soc.* **1962**, 2190−2197. (c) Hoare, D. G.; Waters, W. A. *J. Chem. Soc.* **1962**, 965−971.

(34) KIEs of 1.9−7 have been reported for cerium, vanadium, cobalt, manganese, and chromium-mediated oxidation via metal−alcoholate complexes: (a) Westheimer, F. H.; Nicolaides, N. *J. Am. Chem. Soc.* **1949**, *71*, 25−28. (b) Ardon, M. *J. Chem. Soc.* **1957**, 1811−1815. (c) Litter, J. S.; Waters, W. A. *J. Chem. Soc.* **1959**, 4046−4052.

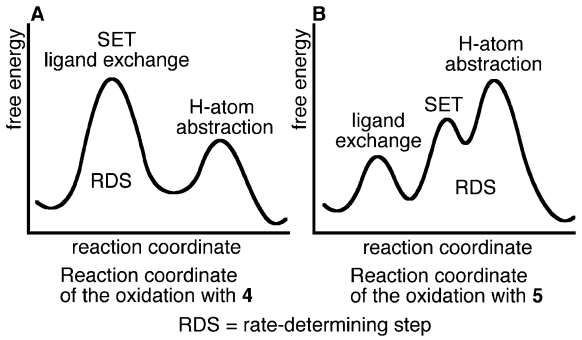

Figure 9. Qualitative free energy diagrams (A and B) for the oxidations with **4** and **5** as catalyst, respectively.

methylene carbon and secondary KIE arising from the nontransferred atom at the methylene carbon. Values of secondary KIE have been found to range between 1.1 and 1.4.[28] Due to the secondary isotope effect, KIE_{intra} is generally larger than KIE_{inter}. The KIE_{intra} and the KIE_{inter} of the oxidation of **26** with **5** agreed with this general trend (entries 6 and 8). On the other hand, the KIE_{inter} of the oxidation of **26** with **4** is larger than the KIE_{intra} (entries 5 and 7). As described above, the kinetics of the oxidation of **26** with **4** showed that the oxidation rate depends on dioxygen concentration and, therefore, the SET contributes to the rate-determining step, while the SET in the oxidation with **5** only partly contributes to the rate-determining step, if any. On the other hand, KIE_{intra} for the SET step should be unity but KIE_{inter} should be larger than unity, if the SET contributes to the rate determination. Thus, KIE_{intra} should reflect only the KIE for hydrogen atom abstraction, while KIE_{inter} should reflect both of the KIEs, the KIEs for SET and for hydrogen atom abstraction. This probably explains why KIE_{inter} is larger than KIE_{intra}, for the oxidation of **26** with **4**, because the SET contributes to the rate-determining step. For the oxidation of **26** with **5**, the SET step contributes to the transition state to a small extent, and KIE_{inter} is smaller than KIE_{intra} (vide supra).

Different from the KIE observed under intra- and intermolecular competition, KIE_{inter} observed under the independent measurement condition gives us important information on the rate-determining step of the oxidation. Based on the above-discussed kinetics of the present oxidation, approximate reaction coordinates for the oxidation with **4** and **5** are described as Figure 9A and 9B, respectively: the ligand exchange and SET steps contribute to the rate-determining step of the oxidation with **4**, while the rate-determining step of the oxidation with **5** is related mainly to hydrogen atom abstraction and partly to the SET steps. In the oxidation with **4** as catalyst, the reactions of **26** and **26**-α,α-d_2 should cross over the transition states for SET and ligand exchange at almost equal rates (Figure 9A).[35] Thus, under intermolecular competitive condition (the oxidation of a mixture of **26** and **26**-α,α-d_2), the relative rate (k_H/k_D) for hydrogen atom abstraction is reflected in their relative oxidation rate (entry 7 and Figure 9A). However, when KIE is measured under independent measurement condition, the k_H/k_D for the hydrogen atom abstraction is hardly reflected in the relative oxidation rate, because the rate of each reaction should be determined by the corresponding rate-determining step and the oxidation rates of **26** and **26**-α,α-d_2 should be almost identical. Indeed, the KIE for the oxidation of **26** and **26**-α,α-d_2 measured with **4** as catalyst under independent measurement condition was small (k_H/k_D = 1.40). On the other hand, the rate-determining step of the oxidation with **5** is the hydrogen-atom abstraction step (Figure 9B), and the k_H/k_D for hydrogen atom abstraction is reflected in their relative oxidation rate, regardless of the measuring methods. Indeed, the KIE for the oxidation with **5** under independent measurement conditions was 2.5, although it was a little smaller than that (k_H/k_D = 3.4) observed under intermolecular competitive condition. This result supports that hydrogen atom abstraction mainly contributes to the rate-determining step of the oxidation with **5** and the KIE of the SET step is minimally reflected in the total KIE. The above-described small KIEs for the oxidation of diol **12a** with **4** and **5** were measured under independent measurement conditions, because of the difficulty of the preparation of stereoisomerically pure **12a**-α,α′-d_2 and of the measurement of the KIE under intermolecular competitive condition. The small KIE for the oxidation with **4** should be expected, because the SET and the ligand exchange are the rate-determining steps for the oxidation of **12a** with **4**. However, the small KIE for the oxidation with **5** is unusual, because the hydrogen atom abstraction is the rate-determining step of the oxidation with **5**. This result strongly suggests that the bond dissociation enthalpy of the C−H bond at the α-methylene becomes weak for some reason (vide infra).

Scheme 4

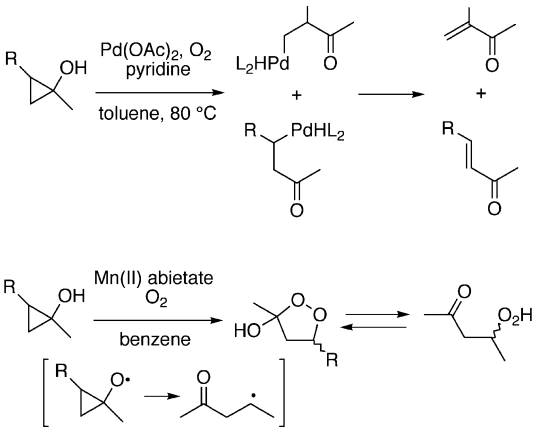

However, as k_H/k_D of 1.6−5.5 has been reported for the oxidation of alcohols via β-hydrogen elimination,[22,24] the possibility that the present oxidation includes a β-hydrogen elimination process cannot be ruled out only by the KIE study.

Oxidation of Cyclopropanol Derivative. Cyclopropanols undergo ring-opening reaction under metal-catalyzed aerobic oxidation; however, the product obtained by the ring-opening depends on the reaction mechanism (Scheme 4).[23] When cyclopropanols are subjected to palladium-catalyzed aerobic oxidation that has been proven to proceed via β-hydrogen elimination, they undergo β-carbon elimination to give ring-opened β-palladioketones, which subsequently undergo β-hydrogen elimination to give unsaturated ketones as the products even in oxygen atmosphere.[36] In contrast, cyclopropanols give β-hydroperoxo ketones via an alkoxy radical and a β-carbonyl

(35) The KIE for the present SET is a secondary one, and it should be much smaller than the primary KIE for hydrogen atom abstraction.

(36) (a) Park, S. B.; Cha, J. K. *Org. Lett.* **2000**, *2*, 147−149. (b) Okumoto, H.; Jinnai, T.; Shimizu, H.; Harada, Y.; Mishima, H.; Suzuki, A. *Synlett* **2000**, 629−630. (c) Nishimura, T.; Ohe, K.; Uemura, S. *J. Am. Chem. Soc.* **1999**, *121*, 2645−2646.

Scheme 5

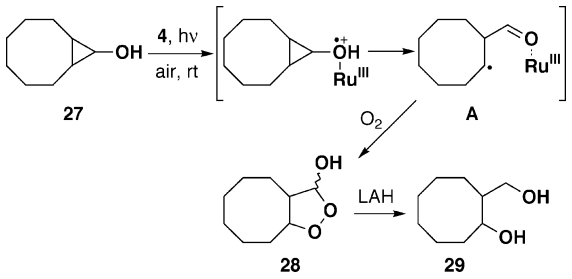

Scheme 6

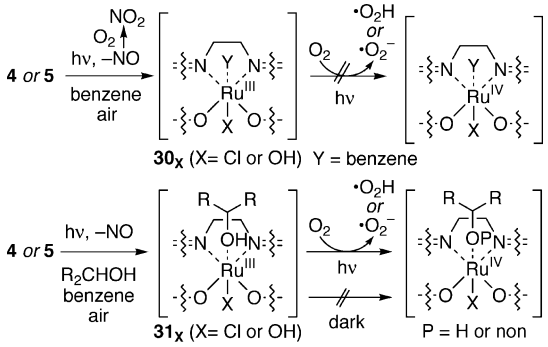

radical,[21c] when they are subjected to aerobic oxidation using one-electron oxidants such as $Fe(acac)_3$ and Mn(II) abietate.[21]

Ru/Al_2O_3 catalyzes oxidation of various alcohols with good yields in oxygen atmosphere.[24] This reaction has been proposed to proceed via a β-hydrogen elimination step, based on radical trap experiments, the analysis of Hammett plots, and the fact that the skeletal isomerization of a cyclopropyl ring used as a radical clock does not proceed at all. To explore whether the oxygen-radical intermediate participates in the present oxidation or not, we examined aerobic oxidation of *exo*-bicyclo[6.1.0]-nonan-9-ol (**27**)[37] using **4** as the catalyst, and 10,11-dioxabicyclo-[6.3.0]undecan-9-ol (**28**) that should be formed via trapping of a radical species (**A**) by molecular oxygen or superoxide was found to be the major product. The structure of compound **28** was determined by ^1H NMR and elementary analyses and further confirmed by chemical correlation to diol **29**[38] (Scheme 5). The oxidation with **5** as the catalyst also gave **28** as the major product, suggesting that the present oxidation proceeds through a radical intermediate, irrespective of the nature of the apical ligand of the catalyst.

UV−Visible Spectroscopic Studies under Photolysis Conditions. It has been proven that photoirradiation promotes dissociation of the apical nitrosyl ligand and this dissociation is a reversible process.[7c] Nitrogen monoxide is, however, oxidized in air to nitrogen dioxide that is equilibrated with dinitrogen tetraoxide. Thus, it was considered that irradiation of (ON)Ru(salen) complex such as **4** in air would provide a denitrosylated Ru(salen) complex $\mathbf{30_{Cl}}$ (Scheme 6).[27] Indeed, when a benzene solution of **4** was irradiated, the color of the solution changed from red to dark greenish-red, and the IR absorption signal (1819 cm^{-1}) of the nitrosyl group diminished gradually and disappeared completely within 12 h.[39] We were intrigued by the catalytic activity of the denitrosylated complex $\mathbf{30_{Cl}}$, and **12a** was added to its solution in the dark. Soon after the addition of **12a**, the color of the solution changed from dark greenish-red to wine-red, but the aerobic oxidation did not proceed in the dark. This result suggested that **12a** is swiftly coordinated to $\mathbf{30_{Cl}}$, but the oxidation of the alcohol-bound Ru^{III} species $\mathbf{31_{Cl}}$ does not occur in the dark. However, when the mixture was re-irradiated, the aerobic oxidation occurred with enantioselectivity of 50% ee that was similar to the selectivity (55% ee) observed with fresh **4** in C_6H_6. This further suggested that irradiation promoted not only the dissociation of the apical ligand but also the oxidation of $\mathbf{31_{Cl}}$. The λ_{max} values of complexes **4** and $\mathbf{30_{Cl}}$ were 467 and 420 nm, respectively. Thus, the dissociation of the apical ligand of **4** was traced with UV/visible spectroscopy.[7b−d] The analysis demonstrated that complex **4** underwent isosbestic transformation to give $\mathbf{30_{Cl}}$ and the half-life of **4** was 27 s (Figure 10a). After 3 min, complex **4** was completely converted into $\mathbf{30_{Cl}}$. However, it is noteworthy that, if the irradiation was stopped, the $\mathbf{30_{Cl}}$ that was generated in the absence of **12a** reverted to **4** rapidly for the first few seconds and then slowly (Figure 10b). This suggested that the nitrosyl group remaining in the solution was recombined with the ruthenium ion rapidly, while the nitrosyl group diffused in the air was mostly oxidized and a part of it was recombined with the ion slowly. This also suggested that $\mathbf{30_{Cl}}$ could not be oxidized to the corresponding Ru^{IV} species in the absence of **12a**.

On the other hand, when the solution of **4** was irradiated in the presence of **12a**, recombination of the dissociated nitrosyl group was not observed at interruption of the irradiation, because **12a** was immediately coordinated to the metal center after the dissociation (Figures 10c). Thus, the ruthenium ion is free of the nitrosyl group during the oxidation, except in the very early stage of the reaction, and oxidation occurs on the ruthenium ion under irradiation. A similar phenomenon was also observed in the experiment with **5** as the catalyst: the oxidation using the corresponding denitrosylated complex $\mathbf{30_{OH}}$ showed enantioselectivity of 58% ee, while enantioselectivity of the oxidation with fresh **5** was 62% ee. The half-life of **5** was 3 min, and complex **5** was completely converted into $\mathbf{30_{OH}}$ within 35 min. Because the reaction with **5** is slow (vide infra), the ruthenium ion is also free of the nitrosyl group during the oxidation, except in the early stage of the reaction. It is noteworthy that complex $\mathbf{31_{OH}}$ does not also undergo dehydrogenation reaction without irradiation.

The Catalytic Cycle for the Present Reaction. (i) The Previously Proposed Catalytic Cycle. We had proposed a catalytic cycle for the present Ru(salen)-catalyzed aerobic oxidation based on preliminary experiments, kinetic resolution,[6a] and oxidative coupling of 2-naphthol[6b] with **6** as catalyst (Scheme 7):[7a,8a] the reaction starts with dissociation of the apical nitrosyl ligand under photoirradiation, which is accompanied by alcohol coordination. The resulting Ru^{III} species **31** undergoes single electron transfer (SET) to dioxygen, giving a Ru^{IV} species **32a** that is resonanced with Ru^{III}-bound oxygen radical species **33a** via radical delocalization. Hydrogen atom and proton transfers from the cationic radical species give the ketone-anchoring Ru^{III} species **34** that undergoes ligand exchange to

(37) (a) Danheiser, R. L.; Savoca, A. C. *J. Org. Chem.* **1985**, *50*, 2401−2403. (b) Schöllkopf, U.; Paust, J.; Azrak, A. A.; Schumacher, H. *Chem. Ber.* **1966**, *99*, 3391−3401.

(38) (a) Uchida, A.; Maeda, T.; Matsuda, S. *Bull. Chem. Soc. Jpn.* **1973**, *46*, 2512−2515. (b) Felföldi, K.; Bartók, M. *ACH − Models Chem.* **1994**, *131*, 535−540.

(39) The oxidation of NO by air is not very fast: Després, J.; Elsener, M.; Koebel, M.; Kröcher, O.; Schnyder, B.; Wokaun, A. *Appl. Catal., B* **2004**, *50*, 73−82. The mechanism of the present NO oxidation is unclear.

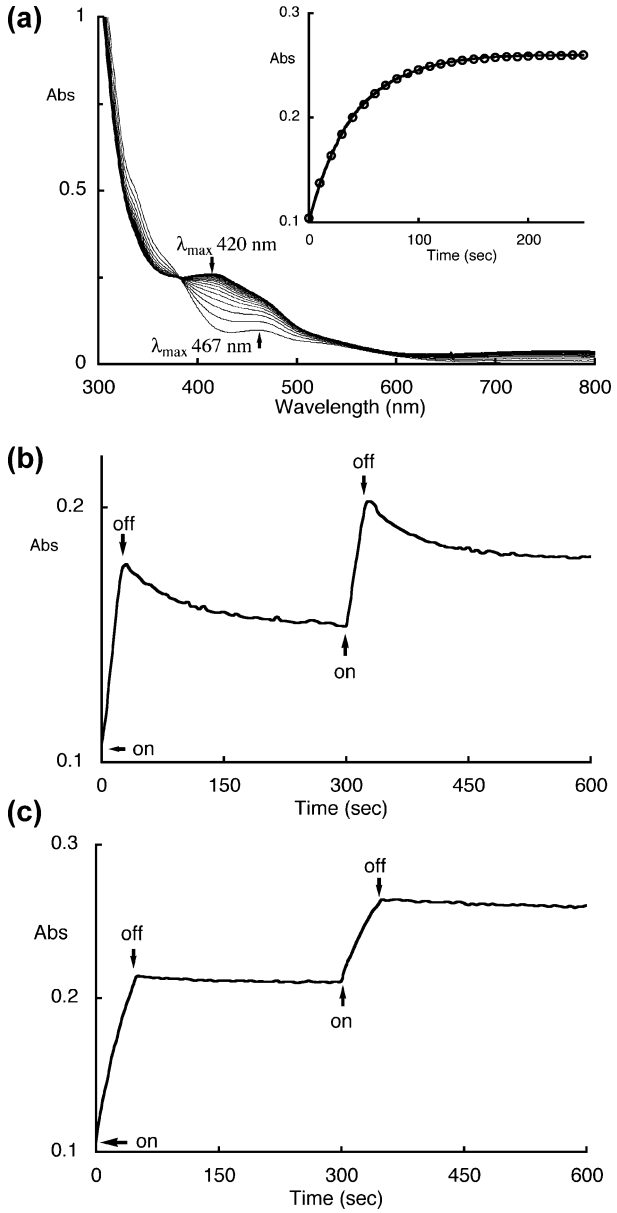

Figure 10. (a) Spectral changes observed for catalyst **4** during continuous photolysis (benzene solution; [Ru] = 2.0×10^{-5} mol L^{-1}). The absorbance was recorded every 10 s. Inset: Increase of the absorbance at 420 nm and the fit to an exponential function (○). (b) Spectral changes observed for intermittent photolysis of catalyst **4** at 420 nm (benzene solution; [Ru] = 2.0×10^{-5} mol L^{-1}). The solution was irradiated for 25 s, and then stirred in the dark for 275 s. (c) Spectral changes observed for intermittent photolysis of catalyst **4** in the presence of *meso*-diol **12a** at 420 nm (benzene solution; [Ru] = 2.0×10^{-5} mol L^{-1}, [**12a**] = 0.2 mol L^{-1}). The solution was irradiated for 50 s, and then stirred in the dark for 250 s.

regenerate the Ru^{III} species **31**, concluding the catalytic cycle. Although the nitrosyl dissociation under irradiation has been clearly proven by the back-reaction of NO with Ru^{III}(salen)-Cl,[7c] adequacy of the proposed catalytic cycle was examined with the above-described kinetic and KIE data and the results of the oxidation of cyclopropanols.

(ii) Identification of the Catalytic Cycle with Kinetic and KIE Data and the Results of the Oxidation of Cyclopropanols. The above-described UV−visible spectroscopic studies under photolysis conditions demonstrated that the formation of the alcohol-bound Ru^{III}(salen) species **31** is very rapid and the catalytic cycle starts from **31**. Furthermore, the kinetic studies

Scheme 7

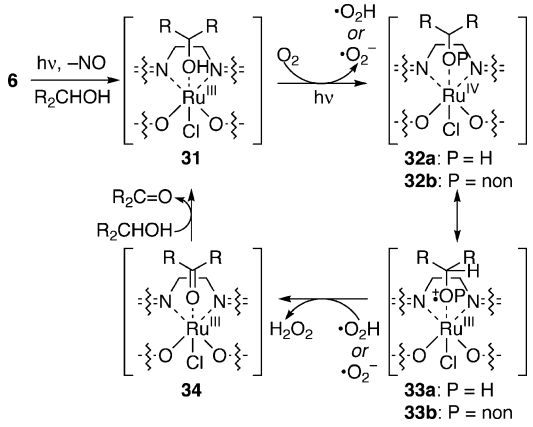

clarified that the rate of the oxidation of **12a** with complex **4** showed first-order dependence on catalyst, diol, and dioxygen concentrations, respectively, while the rate of the oxidation with **5** was found to be first-order dependent on the catalyst concentration but the dependence on dioxygen concentration was 0.42 (vide supra). These facts mean that the catalyst, diol, and dioxygen participate in the rate-determining step of the oxidation with **4** and that the ligand-exchange and the SET steps contribute to the rate-determining step, while hydrogen atom abstraction from a catalyst-diol complex mainly contributes to the rate-determining step of the oxidation with **5** and the SET step partly contributed to the rate-determining step. The observed kinetics of the oxidation of **12a** with complex **4** are inconsistent with the proposed catalytic cycle (vide infra). On the other hand, the H/D relative reaction rate (1.34) for the oxidation of **12a** with **4** determined under independent measurement conditions is consistent with the above kinetics of the oxidation, taking into account the reaction coordinate of the oxidation (Figure 9**A**). However, the small k_H/k_D (1.55) value observed for the oxidation of **12a** with **5** means that the k_H/k_D value for the hydrogen atom abstraction is intrinsically small, because it is the rate-determining step, and the dissociation enthalpy of the C−H bond at the methylene carbon is small. The cleavage of the C−H bond vicinal to a radical atom is facilitated due to the HOMO−SOMO interaction. Thus, the observed KIE suggests participation of **33** that carries a radical oxygen atom, in the oxidation of **12a**.

The kinetics of the oxidation of **26** with **4** and **5** are almost identical to those of the oxidation of **12a** with **4** and **5**, respectively. Thus, the SET and ligand exchange steps contribute to the rate-determining step of the oxidation with **4**, while the hydrogen atom abstraction step mainly contributes to the rate-determining step of the oxidation with **5**. This result agreed well with the above KIE study using **26** as substrate under intra- and intermolecular competition and independent measurement conditions (Figure 9). The studies on kinetics and KIE, however, demonstrated that radical distribution depends on the substrate used (Scheme 6). The intramolecular KIE values (6.18 and 5.23) observed in the oxidation of **26** agreed with the usual methylene C−H bond cleavage[28−32] and are too large for hydrogen atom transfer from a cation radical intermediate (**33**→**34**) (vide infra). Although we had proposed the participation of a cationic oxygen radical species **33** on the basis of the study of the oxidative coupling of 2-naphthol, the KIE values suggest the participation of another cationic oxygen radical species **35** that undergoes

Scheme 8

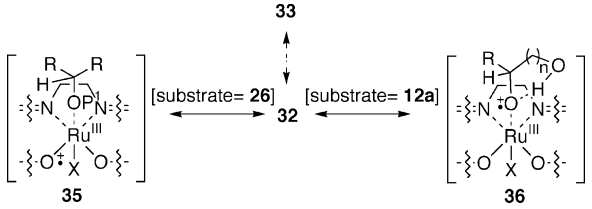

Scheme 9

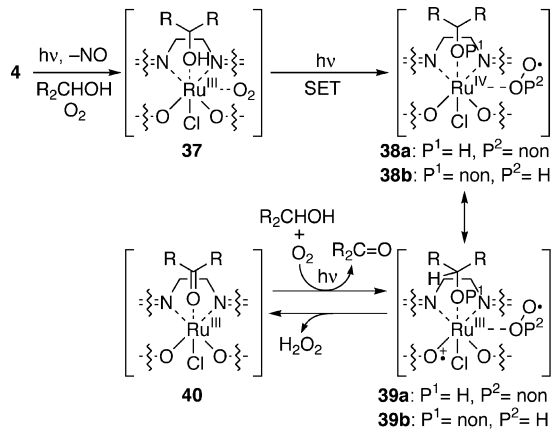

hydrogen atom transfer, for this oxidation (Scheme 8). Taking into account oxidation potentials of phenol and alcohol, the contribution of **35** in radical distribution is considered to be larger than that of **33**. A similar mechanism has been proposed for Cu(II)-Schiff base-catalyzed aerobic oxidation of alcohols.[31]

The above discussion raises a question of why the oxidation of **12a** proceeds through a cationic oxygen radical species **33**. In connection with this question, it has been reported that biphenolic compounds, in which two phenolic hydroxy groups are hydrogen-bonded, show remarkably low ionization potential as compared to phenol. This phenomenon has been attributed to stabilization of a cation radical species by hydrogen bond formation.[40] Because **12a** is expected to make an intramolecular hydrogen bond very easily, the participation of a species **36** in the oxidation of **12a** is likely, and this agrees with the above discussion on the participation of **33** in the oxidation.

The above-described oxidation of cyclopropanol indicated the participation of a cation radical intermediate that corresponds to **33**. The cyclopropyl ring stabilizes a neighboring radical. For example, it has been reported that treatment of methylcyclopropane with a *tert*-butoxy radical gives the corresponding cyclopropylcarbinyl radical.[41a] According to the QCISD/cc-pVDZ calculation, stabilization of the cyclopropoxy radical is ca. 5 kcal/mol.[41b] Furthermore, the cyclopropoxy radical has no barrier against ring opening and the oxidation of cyclopropanol is very likely to proceed through a cyclopropoxy radical.

(iii) The Revised Catalytic Cycles for the Oxidation of Alcohols with 4 or 5 as Catalyst. The experimental results described in the preceding section revealed that the mechanism of the present oxidation varies with the substrate and the catalyst

Scheme 10

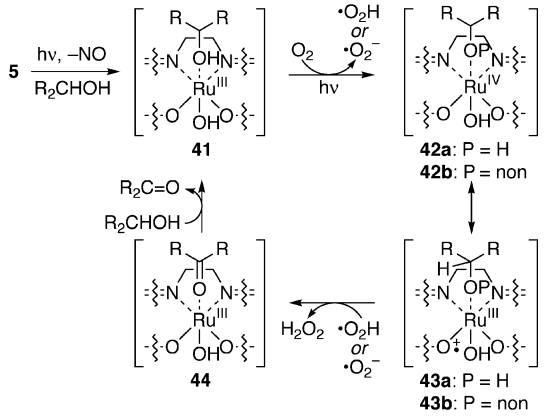

Scheme 11

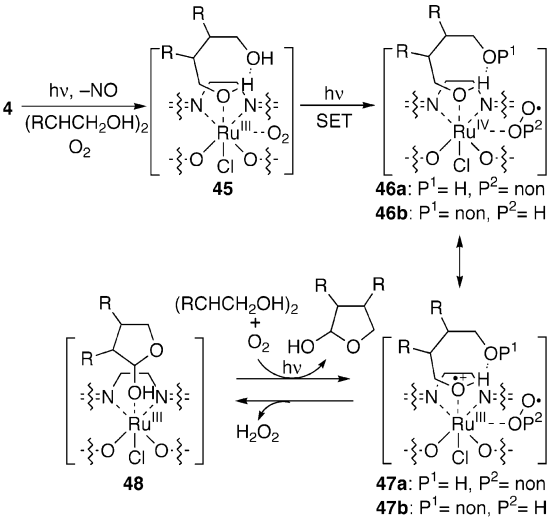

Scheme 12

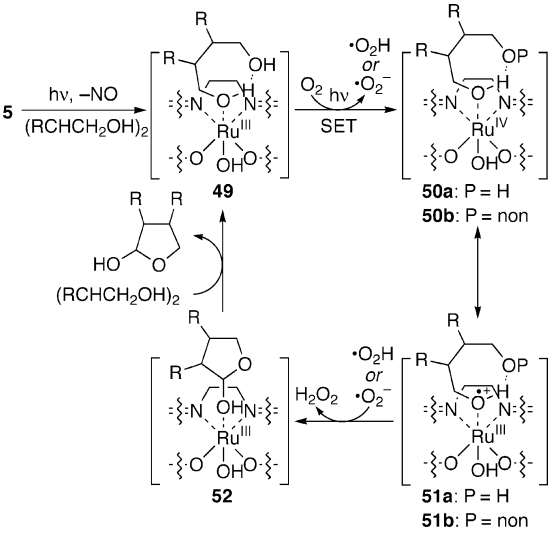

used. The catalytic cycles proposed for each oxidation of mono-ols and diols on the basis of the above results are given in Schemes 9−12. Scheme 9 describes the catalytic cycle for the oxidation of mono-ols with **4**. The kinetic and KIE studies demonstrate that the reaction rate depends on the substrate, catalyst, and dioxygen concentrations, and, therefore, the ketone−alcohol exchange and the SET contribute to the rate-determining step. Thus, the oxidation is considered to proceed

(40) (a) Akahori, H.; Morita, K.; Nishijima, A.; Mitsuhashi, T.; Ohkubo, K.; Fukuzumi, S. *J. Soc. Photogr. Sci. Technol. Japan* **2003**, *66*, 491−496. (b) Akahori, H.; Morita, K.; Nishijima, A.; Mitsuhashi, T.; Ohkubo, K.; Fukuzumi, S. *J. Imaging Sci. Technol.* **2003**, *47*, 124−132.

(41) (a) Kochi, J. K.; Krusic, P. J.; Eaton, D. R. *J. Am. Chem. Soc.* **1969**, *91*, 1877−1879. (b) Cooksy, A. L.; King, H. F.; Richardson, W. H. *J. Org. Chem.* **2003**, *68*, 9441−9452.

through a ternary Ru^{IV}-alcohol-dioxygen complex **38**. The coordination of dioxygen should facilitate the SET from the ruthenium ion to dioxygen, and probably dioxygen coordination is coupled with SET [**37** or **40**→**38**(↔**39**)]. It is unclear which, the peroxy or the phenoxy radical, abstracts the hydrogen atom. It is noteworthy that a ternary Ru^{IV}-olefin-dioxygen complex has been proposed as the intermediate of Ru^{III}(saloph)-catalyzed aerobic epoxidation based on the kinetic study:[42] the rate of the epoxidation depends on the catalyst, olefin, and dioxygen concentrations. These ternary Ru species require the participation of a seven-coordinated Ru species. A seven-coordinated Ru^{IV} complex has been characterized.[43] However, the possibility cannot be ruled out that the reduced dioxygen is dissociated as $\bullet O_2^-$ or •OOH from the ruthenium ion before the hydrogen atom transfer.

In the case of the oxidation of mono-ols with **5**, the KIE study also supports the participation of a phenolic cationic radical species **43**, instead of **33** (X = OH).[31] Furthermore, the KIE and kinetic studies demonstrate that the hydrogen atom abstraction step mainly contributes to the rate-determining step and the SET step partly contributes to the rate-determining step. These experimental results are consistent with the catalytic cycle described in Scheme 10. However, the possibility cannot be ruled out that hydrogen atom transfer is coupled with electron and proton transfers.[31]

For the oxidation of **12a** with **4**, kinetic and KIE studies revealed that the SET and ligand-exchange steps contribute to the rate-determining step, and, therefore, participation of a ternary Ru^{IV}-alcohol-dioxygen complex is expected. Although there is no direct evidence of the participation of a cation radical **47**, its participation is likely because the stabilization of **47** can be expected in this oxidation (vide supra).[40] Based on these results, the following catalytic cycle is proposed for this oxidation (Scheme 11). In analogy with the catalytic cycle for the oxidation of mono-ols with **4**, we cannot rule out the possibility that dioxygen coordination is coupled with SET [**48**→**47**(↔**46**)] and that the reduced dioxygen is dissociated as $\bullet O_2^-$ or •OOH from the ruthenium ion before the hydrogen atom transfer.

In contrast, the kinetic study of the oxidation of **12a** with **5** indicated that the rate-determining step for the oxidation with **5** is hydrogen atom abstraction, although SET also partially contributes to it. Although the KIE of the oxidation is as small as 1.55, it is larger than the secondary KIE. These results suggest that the oxidation of diols with **5** follows the catalytic cycle through hydrogen bond-stabilized cationic radical species **51** (Scheme 12).

Some Other Mechanisms Previously Proposed for Ruthenium-Catalyzed Oxidation of Alcohols. Various oxidations of alcohols using ruthenium complexes as catalyst have been reported.[25] Besides the mechanism through hydrogen atom transfer, mechanisms via β-hydrogen elimination[24,44] and hydride transfer[45] have been proposed for these reactions. However, from the result of the cyclopropanol oxidation, these mechanisms are unlikely for the present oxidation. The oxidation does not give the product expected from β-hydrogen elimination (vide supra). On the other hand, the oxidation of cyclopropanol via hydride transfer should give a transition state of high energy, leading to the formation of cyclopropanone as a primary product, and it is expected to be a slow reaction. However, the oxidation of cyclopropanol **27** is ca. 8 times faster than the oxidation of **12a** and **26**. Furthermore, the reported KIEs (ca. 5−7)[34,45] for hydride transfer do not agree with the KIE of the oxidation of **12a**, although the KIEs are consistent with the KIE of the oxidation of **26**. However, the idea that hydride transfer is only applicable to the oxidation of **26** is unlikely, based on the present kinetic studies indicating that the reactions of **12a** and **26** occur in a similar mechanism (vide supra). In addition to the above-discussed mechanisms, some ruthenium-catalyzed oxidations of alcohols have been proposed to proceed via a Ru(=O) species.[46] However, participation of a Ru(=O) species in the present oxidation is unlikely, taking into account the following experimental results: the oxidation products of cinnamyl alcohol catalyzed by **7** with tetramethylpyrazine *N*,*N*′-dioxide in air varied with the light source used.[6a] When the reaction was carried out using an incandescent lamp as the light source, it produced a mixture of the epoxide and cinnamaldehyde in a 1:3 ratio; however, cinnamaldehyde was exclusively obtained when a more powerful light source, a halogen lamp, was used. These results clearly demonstrate that the catalytic cycles for the present oxidation include a photoaccelerated SET step. It has been reported that treatment of ruthenium complexes with a pyridine *N*-oxide derivative gives the corresponding Ru(=O) species[47] and the Ru(=O) species undergo epoxidation.[48] These results and the reports suggest that an SET process competes with the formation of a Ru^{V}(=O) species in the oxidation of cinnamyl alcohol (Scheme 13). When the reaction is carried out using a stronger light source, the rate of the SET process is accelerated and the generation of the Ru^{V}(=O) species is relatively reduced.[7a] It is reasonable to conclude that the present oxidation in the absence of *N*-oxide does not proceed via a Ru^{V}-(=O) species.

Inspection of the Revised Mechanisms with Other (ON)-Ru(salen)-Catalyzed Oxidation. The present mechanistic studies disclosed that all of the catalytic cycles include alcohol (or alkoxide)-bound Ru^{III} species **37**, **41**, **45**, and **49**, irrespective of the catalyst and the substrate used (Schemes 9−12). This indicates that the alcohols that cannot coordinate with the ruthenium ion could not be oxidized under the present conditions. Complex **6** catalyzed oxidative kinetic resolution of various racemic secondary alcohols in air under irradiation.[6a] However, 1-phenyl-2,2-dimethylpropan-1-ol bearing a bulky *tert*-butyl group attached to the carbinol carbon was completely unreactive under the condition. This is probably attributed to the fact that the presence of the bulky *tert*-butyl group hampers the coordination of the hydroxyl group to the Ru(III) ion. Furthermore, an (ON)Ru(salen) complex bearing 1,1,2,2-tet-

(42) Saloph = bis(salicylaldehyde)-*o*-phenylenediiminato. Taquikhan, M. M.; Mirza, S. A.; Rao, A. R.; Sreelatha, C. *J. Mol. Catal.* **1988**, *44*, 107−115.
(43) (a) Given, K. W.; Mattson, B. M.; Pignolet, L. H. *Inorg. Chem.* **1976**, *15*, 3152−3156. (b) Wheeler, S. H.; Mattson, B. M.; Miessler, G. L.; Pignolet, L. H. *Inorg. Chem.* **1978**, *17*, 340−350.
(44) Murahashi, S.-I.; Naota, T.; Ito, K.; Maeda, Y.; Taki, H. *J. Org. Chem.* **1987**, *52*, 4319−4327.
(45) Roecker, L.; Meyer, T. J. *J. Am. Chem. Soc.* **1987**, *109*, 746−754.
(46) (a) Cundari, T. R.; Drago, R. S. *Inorg. Chem.* **1990**, *29*, 3904−3907. (b) Dalal, M. K.; Upadhyay, M. J.; Ram, R. N. *J. Mol. Catal. A: Chem.* **1999**, *142*, 325−332. (c) Che, C.-M.; Cheng, K.-W.; Chan, M. C. W.; Lau, T.-C.; Mak, C.-K. *J. Org. Chem.* **2000**, *65*, 7996−8000. (d) Griffith, W. P. *Chem. Soc. Rev.* **1992**, *21*, 179−185.
(47) Ohtake, H.; Higuchi, T.; Hirobe, M. *Tetrahedron Lett.* **1992**, *33*, 2521−2524.
(48) (a) Groves J. T.; Quinn, R. *J. Am. Chem. Soc.* **1985**, *107*, 5790−5792. (b) Nakata, K.; Takeda, T.; Mihara, J.; Hamada, T.; Irie, R.; Katsuki, T. *Chem.-Eur. J.* **2001**, *7*, 3776−3782.

Scheme 13

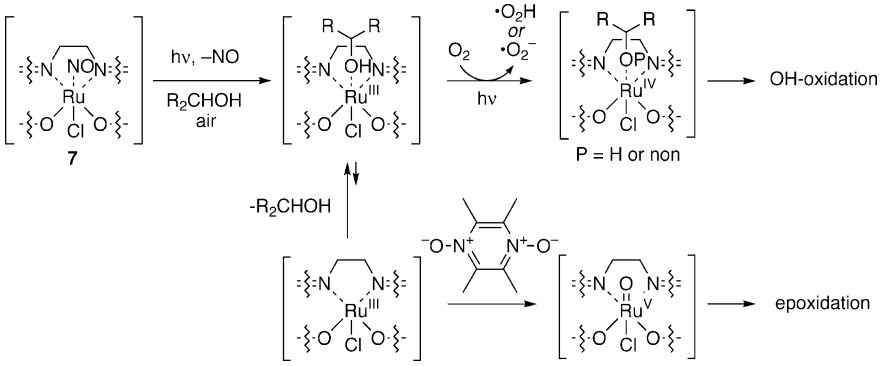

ramethylethylenediamine unit has been found to be an efficient catalyst for selective oxidation of primary alcohol in the presence of secondary alcohol under irradiation.[8] It has been considered that two of the four methyl groups at the diamine unit of this complex adopt pseudoaxial conformation and intercept the approach of a bulkier secondary alcohol to the ruthenium ion.[8a] On the other hand, metal-catalyzed oxidative coupling of 2-naphthol derivatives is known to involve an SET process to afford a metal-bound naphthoxy radical intermediate.[49] Complex **6** also served as the catalyst for enantioselective oxidative coupling of 2-naphthol under aerobic conditions.[6b] Taking into account the ionization potential of 2-naphthol, it is likely that this coupling proceeds through a Ru^{III}-bound naphthoxy radical species.[50] This is compatible with the above discussion on the radical distribution (Scheme 8). It is also noteworthy that the formation of a small amount of 1-nitro-2-naphthol was detected in asymmetric oxidative coupling of 2-naphthol during the oxidative coupling. This also proves that the apical nitrosyl group is dissociated under the present reaction conditions.[6b] Furthermore, it is noteworthy that the present mechanistic studies give a reasonable explanation of the following results: kinetic resolution of racemic secondary alcohols is smoothly effected by using complex **6** that has no axial methyl group at the ethylenediamine unit, as catalyst, while desymmetrization of *meso*-diols is smoothly effected by using complexes (**4**, **5**, **9**, and **10**) that bear axial methyl groups, as catalyst. For the kinetic resolution, participation of a phenoxy radical species **39** forces the ruthenium-bound secondary alkoxide to direct their alkyl moiety to the axially chiral binaphthyl unit of **6** at the hydrogen atom abstraction step. On the other hand, desymmetrization of *meso*-diols proceeds via a hydrogen bond-stabilized radical cation **47** or **51**, and the alkoxide unit on it should be directed away from the bulky binaphthyl unit, if the axial methyl group does not exist. Thus, use of a Ru(salen) complex bearing axial methyl groups is essential for desymmetrization of *meso*-diols, except for the desymmetrization of bulky *meso*-diols.

In conclusion, this study has demonstrated that chiral (ON)-Ru(salen) complexes are efficient catalysts for oxidative desymmetrization of various *meso*-diols, although appropriate choice of the catalyst for each oxidation is required to obtain the optimized enantioselectivity. With the suitable catalysts, high enantioselectivities up to 93% ee were for the first time achieved in aerobic oxidative desymmetrization of *meso*-primary diols. It is noteworthy that the rate-determining step in this oxidative desymmetrization depends on the (ON)Ru(salen) complex used, especially the nature of the apical ligand of the complex. We speculate that the effect of the apical ligand is partly related to an $O_p-Ru_{d\pi}$ electron donation.[51] Thus, the presence of an apical hydroxo ligand may reduce the Lewis acidity and ionization potential of the Ru(III) ion, and, in the oxidation using **5** as catalyst, the SET is not the rate-determining step and dioxygen does not coordinate with the Ru(III) ion. Finally, the finding that the SET and the succeeding events occur on the ruthenium ion explains why (ON)Ru(salen) complexes are a useful catalyst for aerobic asymmetric oxidation of alcohols, although the best substrate for the oxidation varies with the catalyst used.

3. Experimental Section

3.1. General. All reagents and solvents were used as supplied commercially, except for THF and CH_2Cl_2, which were distilled from Na/Ph_2CO and CaH_2, respectively, before use. ^1H and ^{13}C NMR spectra were measured on a JEOL GX-400 spectrometer at 400 and 100 MHz, respectively. All chemical shifts were recorded in δ (ppm) relative to tetramethylsilane (TMS). Melting points were measured with a BUCHI Melting Point B-545 apparatus and are uncorrected. Infrared spectra were measured as a KBr disk or as a thin film using NaCl plate on a SHIMADZU FTIR-8600 spectrophotometer, and only diagnostic absorptions are listed below. UV/visible spectra were measured on SHIMADZU MultiSpec-1500. Optical rotation was measured with a JASCO P-1020 polarimeter. High-resolution EI mass spectra were obtained from a JEOL JMX-SX/SX 102A spectrometer. Enantiomeric excesses were determined by HPLC analysis using SHIMADZU LC-10AT-VP or GLC analysis using SHIMADZU GC-17A (SUPELCO BETA-DEX-225) equipped with an appropriate optically active column, as described in the footnotes to the corresponding tables. TLC analysis was performed on silica gel 60 F_{254}-coated glass plates (Merck). Visualization was accomplished with irradiation of 254 nm UV light or spray of a 12-molybdo(VI)phosphoric acid ethanol solution as the developing agent. Preparation of catalysts and *meso*-diols was carried out under inert atmosphere, unless otherwise specified. Monocyclic *meso*-diols **12** used in this study were prepared in the following conventional manners. *cis*-1,2-Bis(hydroxymethyl)cyclohexane (**12a**) was prepared by LAH reduction of commercial *cis*-1,2-cyclohexanedicarboxylic anhydride (Aldrich). *cis*-1,2-Bis(hydroxymethyl)cyclobutane (**12b**) was obtained by LAH reduction of commercial *cis*-1,2-cyclobutanedicarboxylic acid (Fluka). *cis*-1,2-Bis(hydroxymethyl)cyclopentane (**12c**) was synthesized from commercial *trans*-DL-1,2-cyclopentanedicarboxylic acid (Aldrich) in the following sequence: (i) dehydration at 220 °C and (ii) LAH reduction of the resulting *cis*-1,2-cyclopen-

(49) Whiting, D. A. In *Comprehensive Organic Synthesis*; Trost, B. M., Fleming, I., Pattenden, G., Eds.; Pergamon Press: Oxford, 1991; Vol. 3, pp 659−703.

(50) Kochi, J. K. In *Comprehensive Organic Synthesis*; Trost, B. M., Ed.; Pergamon Press: Oxford, 1991; Vol. 7, pp 849−889.

(51) Chishholm, M. H.; Davidson, E. R.; Huffman, J. C.; Quinlan, K. B. *J. Am. Chem. Soc.* **2001**, *123*, 9652−9664.

tanedicarboxylic anhydride. *cis*-1,2-Bis(hydroxymethyl)cycloheptane (**12d**) was prepared according to Hirashima's protocol with slight modification (Hirashima, T.; Nishiguchi, I.; Ishino, Y.; Komatsu, H.; Iwasaki, Y. *Jpn. Kokai Tokkyo Koho* **1993**, 3 pp. JP05065262; *Chem. Abstr.* **1993**, *119*(*VII*), 830). *cis*-1,2-Bis(hydroxymethyl)-4-cyclohexene (**12e**) was prepared by LAH reduction of commercial *cis*-1,2,3,6-tetrahydrophthalic anhydride (Aldrich). *cis*-1,2-Bis(hydroxymethyl)-cyclohexane-d_4 (**12a**-d_4) was prepared by reduction of commercial *cis*-1,2-cyclohexanedicarboxylic anhydride (Aldrich) using lithium aluminum deuteride (Aldrich, 98 atom % D). 3-Phenylpropanol-1-*d* (**26**-d_1) was prepared by reduction of hydrocinnamaldehyde (Nacalai tesque) using lithium aluminum deuteride. 3-Phenylpropanol-1-d_2 (**26**-d_2) was prepared by reduction of ethyl 3-phenylpropionate using lithium aluminum deuteride.

3.2. Syntheses of (ON$^+$)Ru(II)(salen) Complexes. 3.2.1. Syntheses of (*R*,a*R*)-(ON$^+$)Ru(II)(salen) Complexes 4 and 5. To a solution of (1*R*,2*R*)-1,2-dimethyl-1,2-cyclohexanediammonium dimandelate[13] (**2**, 350 mg, 0.78 mmol) in ethanol (10 mL) were added potassium hydroxide (1.0 M in ethanol, 1.6 mL) and (a*R*)-3-formyl-2-hydroxy-2′-phenyl-1,1′-binaphthyl[12] (580 mg, 1.55 mmol). After being stirred for 12 h at ambient temperature, the resulting mixture was concentrated in vacuo, diluted with CH_2Cl_2, and filtered through a pad of Celite. The filtrate was evaporated under reduced pressure and redissolved in THF (10 mL). To the mixture was added NaH (60% dispersion in mineral oil, 67 mg, 1.65 mmol). After being stirred for 1 h at 60 °C, the mixture was concentrated under vacuum and redissolved in toluene (20 mL). To the solution was added $RuCl_3(NO)(PPh_3)_2$ (888 mg, 1.12 mmol), and the mixture was refluxed for another 20 h. The solution was evaporated under reduced pressure, and the residue was purified by basic silica gel column chromatography (toluene/acetone = 10/1) to give crude **4** and **5**. Each of products was further purified by column chromatography using florisil (100−200 mesh) (*n*-hexane/ethyl acetate = 3/7) to afford **4** (370 mg, 47%) as dark brown crystals and **5** (200 mg, 26%) as brown crystals, respectively.

Complex 4. IR (KBr): 3049, 2936, 1834, 1609, 1576, 1547, 1379, 1317, 1229, 1188, 1146, 1115, 1026, 951, 864, 818, 743, 698 cm^{-1}. ^{1}H NMR ($CDCl_3$): δ 8.25 (s, 1H), 8.16 (d, J = 8.8 Hz, 1H), 8.14 (s, 1H), 8.04 (d, J = 8.5 Hz, 1H), 8.01 (d, J = 8.3 Hz, 1H), 7.88 (d, J = 8.3 Hz, 1H), 7.80 (d, J = 5.6 Hz, 2H), 7.66 (d, J = 8.1 Hz, 1H), 7.65 (d, J = 8.5 Hz, 1H), 7.60 (d, J = 7.8 Hz, 1H), 7.51 (d, J = 8.5 Hz, 1H), 7.47 (dt, J = 5.6, 2.4 Hz, 1H), 7.38 (t, J = 6.7 Hz, 1H), 7.28−7.12 (m, 6H), 7.09−6.99 (m, 4H), 6.58 (dt, J = 14.8, 7.6 Hz, 2H), 6.21 (br t, J = 6.7 Hz, 4H), 6.10 (dt, J = 14.8, 7.6 Hz, 4H), 2.32 (br d, J = 10.3 Hz, 1H), 2.11 (m, 2H), 2.04−1.97 (m, 1H), 1.95−1.75 (m, 4H), 1.70 (s, 3H), 1.03 (s, 3H). Anal. Calcd for $C_{62}H_{48}ClN_3O_3Ru\cdot{}^1/_4CH_2Cl_2$: C, 71.83; H, 4.70; N, 4.04. Found: C, 71.83; H, 4.82; N, 3.93.

Complex 5. IR (KBr): 3539, 3423, 3049, 2947, 2874, 1813, 1612, 1576, 1423, 1379, 1319, 1229, 1188, 1146, 1117, 949, 818, 743, 696 cm^{-1}. ^{1}H NMR ($CDCl_3$): δ 8.16 (m, 3H), 8.10 (s, 1H), 8.00 (d, J = 8.3 Hz, 1H), 7.93 (d, J = 8.3 Hz, 1H), 7.83 (s, 1H), 7.80 (s, 1H), 7.68 (d, J = 8.3 Hz, 1H), 7.64 (d, J = 8.3 Hz, 1H), 7.61 (d, J = 8.3 Hz, 2H), 7.47 (m, 1H), 7.41 (br t, J = 8.1 Hz, 1H), 7.28−7.13 (m, 6H), 7.11−6.99 (m, 4H), 6.60 (t, J = 7.6 Hz, 1H), 6.58 (t, J = 7.3 Hz, 1H), 6.20 (d, J = 7.3 Hz, 2H), 6.15 (d, J = 7.6 Hz, 2H), 6.06 (m, 4H), 2.25 (m, 1H), 2.17 (m, 1H), 2.09 (m, 1H), 2.01 (m, 1H), 1.92−1.75 (m, 4H), 1.63 (s, 3H), 1.04 (s, 3H). HRMS (FAB) *m*/*z* 1001.2784 ([M]$^+$ calcd for $C_{62}H_{49}N_3O_4Ru^+$: 1001.2767).

3.2.2. Synthesis of (*S*,a*R*)-(ON$^+$)Ru(II)(salen) Complex 8. Complex **8** was prepared in a procedure similar to that described for the synthesis of **4**. Complex **8** was obtained as dark brown crystals (17% yield). IR (KBr): 3049, 2999, 1830, 1609, 1576, 1445, 1423, 1377, 1317, 1227, 1186, 1144, 1113, 949, 816, 762, 741, 700 cm^{-1}. ^{1}H NMR ($CDCl_3$): δ 8.36 (s, 1H), 8.22 (s, 1H), 8.10 (d, J = 8.3 Hz, 1H), 8.02 (d, J = 8.1 Hz, 1H), 7.85 (d, J = 8.3 Hz, 1H), 7.79 (s, 1H), 7.72 (s, 1H), 7.66 (d, J = 8.1 Hz, 1H), 7.61 (d, J = 8.3 Hz, 1H), 7.52 (d, J = 8.3 Hz, 2H), 7.46 (br t, J = 8.1 Hz, 1H), 7.31 (d, J = 8.3 Hz, 1H), 7.23−6.91 (m, 11H), 6.76 (br t, J = 7.3 Hz, 1H), 6.70 (br t, J = 7.3 Hz, 1H), 6.54 (br d, J = 7.1 Hz, 2H), 6.45 (br t, J = 7.8 Hz, 2H), 6.38 (br t, J = 7.8 Hz, 2H), 6.30 (br d, J = 7.1 Hz, 2H), 2.37 (m, 1H), 2.16 (m, 2H), 2.02 (m, 1H), 1.95−1.81 (m, 4H), 1.74 (s, 3H), 1.13 (s, 3H). Anal. Calcd for $C_{62}H_{48}ClN_3O_3Ru\cdot H_2O$: C, 71.77; H, 4.86; N, 4.05. Found: C, 71.71; H, 4.93; N, 3.84. HRMS (FAB) *m*/*z* 1019.2442 ([M]$^+$ calcd for $C_{62}H_{48}ClN_3O_3Ru^+$: 1019.2428).

3.2.3. Syntheses of (*S*,a*S*)-(ON$^+$)Ru(II)(salen) Complexes 9 and 10. To a solution of (1*S*,2*S*)-1,2-dimethyl-1,2-cyclohexanediammonium dimandelate (*ent*-**2**, 100 mg, 0.22 mmol) in ethanol (3.0 mL) were added potassium hydroxide (1.0 M in ethanol, 0.47 mL) and (a*S*)-3-formyl-2-hydroxy-2′-(4-biphenylyl)-1,1′-binaphthyl (**53**, 196 mg, 0.44 mmol). After being stirred for 19 h at ambient temperature, the resulting mixture was concentrated in vacuo, diluted with CH_2Cl_2, and filtered through a pad of Celite. The filtrate was evaporated under reduced pressure, and the resulting crude diimine (180 mg) was dissolved in THF (3.0 mL) and treated with NaH (60% dispersion in mineral oil, 16 mg, 0.40 mmol). After being stirred at 60 °C for 1 h, the mixture was concentrated under vacuum. The residue was dissolved in toluene (3.0 mL) and treated with $RuCl_3(NO)(PPh_3)_2$ (205 mg, 0.27 mmol). After being refluxed for 16 h, the solution was evaporated under reduced pressure and the residue was chromatographed on basic silica gel (toluene/acetone = 10/1) to give crude **9** and **10**. Each of the products was purified by column chromatography using florisil (100−200 mesh) (*n*-hexane/ethyl acetate = 3/7) to afford **9** (36 mg, 17%) and **10** (59 mg, 28%) as dark brown crystals, respectively.

Complex 9. IR (KBr): 3049, 2934, 2876, 1832, 1609, 1576, 1485, 1379, 1317, 1227, 1186, 1146, 1113, 949, 814, 741, 694 cm^{-1}. ^{1}H NMR ($CDCl_3$): δ 8.25 (s, 1H), 8.21 (d, J = 8.3 Hz, 1H), 8.13 (s, 1H), 8.06 (d, J = 8.3 Hz, 1H), 7.99 (d, J = 8.3 Hz, 1H), 7.83−7.76 (m, 4H), 7.69 (d, J = 7.8 Hz, 1H), 7.60−7.51 (m, 3H), 7.32−7.06 (m, 19H), 6.99 (t, J = 7.8 Hz, 2H), 6.48 (d, J = 8.1 Hz, 2H), 6.34 (d, J = 8.1 Hz, 2H), 6.27 (m, 4H), 2.31 (m, 1H), 2.10 (m, 2H), 2.04−1.71 (m, 4H), 1.68 and 0.99 (each s, 3H). HRMS (FAB) *m*/*z* 1171.3062 ([M]$^+$ calcd for $C_{74}H_{56}ClN_3O_3Ru^+$: 1171.3054).

Complex 10. IR (KBr): 3543, 2997, 2937, 1809, 1611, 1578, 1485, 1445, 1317, 1294, 1229, 1188, 1144, 1113, 949, 816, 768, 741, 694 cm^{-1}. ^{1}H NMR ($CDCl_3$): δ 8.20 (d, J = 8.3 Hz, 1H), 8.16 (s, 1H), 8.13 (d, J = 8.6 Hz, 1H), 8.08 (s, 1H), 8.05 (d, J = 8.1 Hz, 1H), 7.95 (d, J = 7.8 Hz, 1H), 7.85 (s, 1H), 7.80 (s, 1H), 7.72−7.62 (m, 4H), 7.53 (dt, J = 8.1, 1.5 Hz, 1H), 7.46 (br t, J = 7.8 Hz, 1H), 7.35−7.09 (m, 18H), 7.05−7.00 (m, 2H), 6.33−6.27 (m, 8H), 2.25−2.13 (m, 2H), 2.08−2.05 (m, 1H), 1.96 (m, 1H), 1.89−1.75 (m, 4H), 1.54 (s, 3H), 1.00 (s, 3H). Anal. Calcd for $C_{74}H_{57}N_3O_4Ru\cdot CH_2Cl_2$: C, 72.75; H, 4.80; N, 3.39. Found: C, 72.53; H, 4.89; N, 3.35.

3.2.4. Synthesis of (*S*,a*S*)-(ON$^+$)Ru(II)(salen) Complex 11. Complex **11** was synthesized from (a*S*)-3-formyl-2-hydroxy-2′-(4-*tert*-buthydiphenylsilylphenyl)-1,1′-binaphthyl[52] and (1*S*,2*S*)-1,2-dimethyl-1,2-cyclohexanediammonium dimandelate[13] in a manner similar to that described for the synthesis of **4** and **5**. In this experiment, however, only hydroxo complex **11** was obtained as dark brown crystals (34% yield). IR (KBr): 3543, 3427, 3049, 2932, 2856, 1811, 1612, 1578, 1547, 1445, 1425, 1383, 1319, 1290, 1229, 1190, 1146, 1107, 1076, 1022, 951, 814, 743, 700 cm^{-1}. ^{1}H NMR ($CDCl_3$): δ 8.21 (s, 1H), 8.16 (t, J = 7.8 Hz, 2H), 8.09 (s, 1H), 7.94 (d, J = 7.8 Hz, 1H), 7.88 (d, J = 8.3 Hz, 1H), 7.86 (s, 1H), 7.80 (s, 1H), 7.65 (d, J = 8.3 Hz, 1H), 7.62 (d, J = 8.3 Hz, 1H), 7.56 (d, J = 8.5 Hz, 1H), 7.55 (d, J = 8.3 Hz, 1H), 7.36−6.92 (m, 30H), 6.87 (d, J = 8.5 Hz, 1H), 6.71 (br t, J = 8.3 Hz, 1H), 6.43 (d, J = 8.1 Hz, 2H), 6.29 (d, J = 8.1 Hz, 2H), 6.21 (d, J = 8.1 Hz, 2H), 6.02 (d, J = 8.1 Hz, 2H), 2.26 (m, 1H), 2.17 (m, 1H), 2.10 (m, 1H), 2.04 (s, 3H), 1.99 (m, 1H), 1.95−1.75 (m, 4H), 1.00 (s, 3H), 0.92 (s, 9H), 0.87 (s, 9H). HRMS (FAB) *m*/*z* 1477.5148 ([M]$^+$ calcd for $C_{94}H_{85}N_3O_4RuSi_2^+$: 1477.5122).

(52) Hamada, T.; Irie, R.; Mihara, J.; Hamachi, K.; Katsuki, T. *Tetrahedron* **1998**, *54*, 10017−10028.

Complex 17. Dark brown crystals. IR (KBr): 3047, 2934, 2856, 1821, 1614, 1578, 1425, 1319, 1105, 1026, 814, 746, 700 cm^{-1}. ^1H NMR ($CDCl_3$): δ 8.28 (br s, 1H), 8.22 (br s, 1H), 8.13 (d, J = 8.3 Hz, 1H), 7.95 (d, J = 8.3 Hz, 1H), 7.92 (d, J = 8.1 Hz, 1H), 7.87 (s, 1H), 7.79 (s, 1H), 7.74 (d, J = 7.8 Hz, 1H), 7.65 (d, J = 7.8 Hz, 1H), 7.62 (d, J = 8.3 Hz, 1H), 7.56 (d, J = 8.1 Hz, 1H), 7.37 (br d, J = 8.1 Hz, 2H), 7.31−6.98 (m, 27H), 6.92 (m, 3H), 6.81 (d, J = 8.5 Hz, 1H), 6.60 (dq, J = 8.3 Hz, 4H), 6.53 (d, J = 8.1 Hz, 2H), 6.20 (d, J = 8.1 Hz, 2H), 4.04 (br t, J = 11.2 Hz, 1H), 3.03 (br t, J = 11.2 Hz, 1H), 2.59 (m, 2H), 2.00 (br d, J = 11.2 Hz, 1H), 1.91 (br d, J = 11.2 Hz, 1H), 1.66 (m, 1H), 1.41 (m, 1H), 1.26 (m, 2H), 0.96 and 0.90 (each s, 9H). HRMS (FAB) m/z 1467.4492 ($[M]^+$ calcd for $C_{92}H_{80}ClN_3O_3RuSi_2^+$: 1467.4470).

Complex 18. Red brown crystals. IR (KBr): 3547, 3047, 2934, 2856, 1807, 1643, 1614, 1580, 1425, 1321, 1105, 1026, 814, 746, 700 cm^{-1}. ^1H NMR ($CDCl_3$): δ 8.22 (br d, J = 11.5 Hz, 2H), 8.15 (d, J = 8.3 Hz, 1H), 8.11 (d, J = 8.3 Hz, 1H), 7.95 (d, J = 7.8 Hz, 1H), 7.86 (m, 3H), 7.65 (t, J = 8.5 Hz, 2H), 7.49 (t, J = 8.5 Hz, 2H), 7.32−6.87 (m, 31H), 6.82 (t, J = 7.1 Hz, 1H), 6.44 (br t, J = 7.3 Hz, 4H), 6.19 (d, J = 7.3 Hz, 4H), 3.76 (br t, J = 11.5 Hz, 1H), 3.09 (br t, J = 11.5 Hz, 1H), 2.70 (br d, J = 11.5 Hz, 1H), 2.57 (br d, J = 11.5 Hz, 1H), 2.04 (m, 2H), 1.80 (m, 1H), 1.63−1.39 (m, 3H), 0.91 and 0.88 (each s, 9H). HRMS (FAB) m/z 1449.4835 ($[M]^+$ calcd for $C_{92}H_{81}N_3O_4RuSi_2^+$: 1449.4809).

3.3. Syntheses of Optically Active Lactols and Lactones. 3.3.1. (1*R*,6*S*,7*RS*)-7-Hydroxy-8-oxabicyclo[4.3.0]nonane (13a). *meso*-Diol **12a** (14.4 mg, 0.1 mmol) and complex **10** (4.6 mg, 4.0 μmol, 4 mol %) were dissolved in anhydrous $CHCl_3$ (0.5 mL). The solution was stirred at ambient temperature under irradiation with a halogen lamp in air for 7 days. The mixture was directly chromatographed on silica gel (*n*-hexane/ethyl acetate = 1/1) to give the corresponding lactol **13a** (11.4 mg, 80%) as a colorless oil. Compound **13a** was a >95:<5 mixture of isomers diastereomeric at C7. IR (neat): 3383, 2928, 1448, 1047, 997, 908 cm^{-1}. ^1H NMR ($CDCl_3$): δ 5.17 (s, 1H), 4.05 (t, J = 8.0 Hz, 1H), 3.72 (t, J = 8.0 Hz, 1H), 2.63 (d, J = 3.2 Hz, 1H), 2.60−2.50 (m, 1H), 2.08−2.01 (m, 1H), 1.70−1.52 (m, 4H), 1.46−1.38 (m, 2H), 136−1.24 (m, 2H). ^{13}C NMR ($CDCl_3$): δ 102.6, 70.5, 44.9, 35.0, 24.3, 24.1, 23.4, 21.9. Anal. Calcd for $C_8H_{14}O_2$: C, 67.57; H, 9.92. Found: C, 67.50; H, 9.96.

3.3.2. (1*R*,6*S*)-8-Oxabicyclo[4.3.0]nonan-7-one (14a). To a suspension of the lactol **13a** (11.4 mg, 0.08 mmol) and molecular sieves 4A (120 mg) in anhydrous CH_2Cl_2 (0.5 mL) was added pyridinium dichromate (60 mg, 0.16 mmol). The mixture was stirred overnight at room temperature, diluted with *n*-hexane/ethyl acetate (4/1), and filtered through a pad of silica gel. The filtrate was concentrated under reduced pressure. The enantiomeric excess of the resulting lactone **14a** was determined to be 80% ee by GLC analysis. $[\alpha]^{23}_D$ +40.4 (*c* 0.21, $CHCl_3$) [lit.: $[\alpha]^{25}_D$ +48.8 (*c* 0.5, $CHCl_3$)].[3b] IR (neat): 2934, 2856, 1773, 1448, 1375, 1348, 1319, 1275, 1211, 1188, 1161, 1128, 1067, 1040, 986, 939, 914, 849, 712 cm^{-1}. ^1H NMR ($CDCl_3$): δ 4.20 (dd, J = 8.8, 5.1 Hz, 1H), 3.96 (dd, J = 8.8, 1.2 Hz, 1H), 2.64 (dt, J = 6.3, 3.2 Hz, 1H), 2.49−2.43 (m, 1H), 2.13 (br d, J = 12 Hz, 1H), 1.85−1.78 (m, 1H), 1.67−1.58 (m, 3H), 1.30−1.18 (m, 3H). ^{13}C NMR ($CDCl_3$): δ 178.0, 71.7, 39.6, 35.5, 27.3, 23.6, 23.1, 22.7. HRMS (EI) m/z 140.0841 ($[M]^+$ calcd for $C_8H_{12}O_2$: 140.0837).

3.3.3. (1*S*,2*RS*,5*R*)-2-Hydroxy-3-oxabicyclo[3.2.0]heptane (13b). Colorless oil (64% yield). Compound **13b** was a single diastereomer, although the configuration of C2 has not been determined. IR (neat): 3395, 2936, 1292, 1074, 966, 910 cm^{-1}. ^1H NMR ($CDCl_3$): δ 5.35 (s, 1H), 4.04 (dd, J = 9.0, 5.6 Hz, 1H), 3.84 (d, J = 9.0 Hz, 1H), 3.02−2.95 (m, 1H), 2.92−2.86 (m, 1H), 2.55 (br s, 1H), 2.24−2.06 (m, 2H), 1.74−1.64 (m, 2H). ^{13}C NMR ($CDCl_3$): δ 102.9, 73.0, 44.7, 36.6, 23.6, 20.4. Anal. Calcd for $C_6H_{10}O_2$: C, 63.14; H, 8.83. Found: C, 62.96; H, 8.84.

3.3.4. (1*S*,5*R*)-3-Oxabicyclo[3.2.0]heptan-2-one (14b). Colorless oil (74% ee). $[\alpha]^{23}_D$ +88.0 (*c* 0.22, $CHCl_3$) [lit.: $[\alpha]^{25}_D$ +118.7 (*c* 10, $CHCl_3$)].[3b] IR (neat): 2962, 2905, 2866, 1763, 1477, 1439, 1371, 1288, 1236, 1155, 1059, 978, 880, 731 cm^{-1}. ^1H NMR ($CDCl_3$): δ 4.36 (dd, J = 9.5, 6.3 Hz, 1H), 4.24 (dd, J = 9.5, 1.5 Hz, 1H), 3.19 (m, 1H), 3.10 (m, 1H), 2.56 (m, 1H), 2.41 (m, 1H), 2.21−2.07. ^{13}C NMR ($CDCl_3$): δ 180.5, 74.0, 38.1, 34.4, 25.4, 23.6. Anal. Calcd for $C_6H_8O_2$: C, 64.27; H, 7.19. Found: C, 64.30; H, 7.14.

3.3.5. (1*S*,2*RS*,5*R*)-2-Hydroxy-3-oxabicyclo[3.3.0]octane (13c). Colorless oil (78% yield). Compound **13c** was a single diastereomer, although the configuration of C2 has not been determined. IR (neat): 3402, 2949, 1447, 1335, 1049, 1007, 962, 908 cm^{-1}. ^1H NMR ($CDCl_3$): δ 5.22 (s, 1H), 4.19 (dd, J = 8.8, 7.3 Hz, 1H), 3.64 (dd, J = 8.8, 2.5 Hz, 1H), 2.82−2.74 (m, 1H), 2.59 (dt, J = 8.8, 4.9 Hz, 1H), 2.46 (d, J = 2.2 Hz, 1H), 1.84−1.76 (m, 2H), 1.65−1.40 (m, 4H). ^{13}C NMR ($CDCl_3$): δ 104.7, 73.7, 51.3, 42.3, 33.9, 30.9, 26.5. Anal. Calcd for $C_7H_{12}O_2$: C, 65.60; H, 9.44. Found: C, 65.73; H, 9.47. HRMS (EI) m/z 129.0905 ($[M + H]^+$ calcd for $C_7H_{13}O_2$: 129.0916).

3.3.6. (1*S*,5*R*)-3-Oxabicyclo[3.3.0]octan-2-one (14c). Colorless oil (66% ee). $[\alpha]^{23}_D$ +66.5 (*c* 0.95, $CHCl_3$) [lit.: $[\alpha]_D^{25}$ +96.9 (*c* 1, $CHCl_3$)].[3b] IR (neat): 2959, 2910, 2870, 1763, 1481, 1450, 1331, 1263, 1184, 1140, 1101, 1061, 1011, 970, 934, 901, 841, 708 cm^{-1}. ^1H NMR ($CDCl_3$): δ 4.47 (dd, J = 9.5, 7.8 Hz, 1H), 3.99 (dd, J = 9.5, 3.4 Hz, 1H), 3.01 (dt, J = 9.3, 2.4 Hz, 1H), 2.95 (m, 1H), 2.10 (m, 1H), 1.91 (m, 2H), 1.73 (m, 1H), 1.65−1.52 (m, 2H). ^{13}C NMR ($CDCl_3$): δ 180.7, 73.6, 53.5, 44.5, 39.1, 33.9, 30.8, 25.6. Anal. Calcd for $C_7H_{10}O_2$: C, 66.65; H, 7.99. Found: C, 66.65; H, 8.08.

3.3.7. (1*S,7*R**,8*RS*)-8-Hydroxy-9-oxabicyclo[5.3.0]decane (13d).** The product was obtained as a 3:1 mixture of isomers diastereomeric at C8. Absolute configuration of the product has not been determined. Colorless oil (80% yield). IR (neat): 3358, 2916, 2851, 1456, 1339, 1248, 1092, 997, 930, 878 cm^{-1}. ^1H NMR of the major isomer ($CDCl_3$): δ 5.10 (t, J = 2.9 Hz, 1H), 4.22 (t, J = 8.4 Hz, 1H), 3.52 (dd, J = 8.4, 5.9 Hz, 1H), 2.66 (d, J = 2.9 Hz, 1H), 2.63−2.53 (m, 1H), 2.19 (ddt, J = 12, 9.0, 2.9 Hz, 1H), 1.94−1.70 (m, 5H), 1.60−1.18 (m, 5H). ^1H NMR of the minor isomer ($CDCl_3$): δ 5.35 (m, 1H), 4.09 (t, J = 8.5 Hz, 1H), 3.62 (t, J = 8.5 Hz, 1H), 2.47 (d, J = 2.9 Hz, 1H, −OH), 2.32 (m, 2H), 1.92−1.15 (m, 10H). ^{13}C NMR of the major isomer ($CDCl_3$): δ 105.6, 73.9, 51.3, 41.5, 31.4, 30.6, 29.0, 28.5, 28.2. ^{13}C NMR of the minor isomer ($CDCl_3$): δ 100.1, 72.7, 48.1, 41.9, 31.5, 30.2, 30.0, 28.1, 25.2. HRMS (EI) m/z 155.1072. Found for diastereomeric mixture ($[M - H]^+$ calcd for $C_9H_{15}O_2$: 155.1072).

3.3.8. (1*S,7*R**)-9-Oxabicyclo[5.3.0]decan-8-one (14d).** Colorless oil (63% ee). Absolute configuration of the product has not been determined. $[\alpha]^{24}_D$ +38.3 (*c* 0.35, $CHCl_3$). IR (neat): 2924, 2853, 1763, 1481, 1458, 1383, 1281, 1169, 1030, 993, 912, 876, 808, 700 cm^{-1}. ^1H NMR ($CDCl_3$): δ 4.39 (dd, J = 9.3, 7.8 Hz, 1H), 3.90 (dd, J = 9.3, 5.4 Hz, 1H), 2.79 (dt, J = 9.8, 4.4 Hz, 1H), 2.72 (m, 1H), 2.06 (m, 1H), 1.94−1.72 (m, 4H), 1.69−1.48 (m, 2H), 1.40−1.25 (m, 3H). ^{13}C NMR ($CDCl_3$): δ 179.9, 73.0, 44.3, 40.0, 31.3, 31.0, 28.2, 28.1, 27.52. HRMS (EI) m/z 154.1003 ($[M]^+$ calcd for $C_9H_{14}O_2^+$: 154.0994).

3.3.9. (1*R*,6*S*,7*RS*)-7-Hydroxy-8-oxabicyclo[4.3.0]non-3-ene (13e). Compound **13e** was a single diastereomer, although the configuration of C7 has not been determined. Colorless oil (68% yield). IR (neat): 3387, 3024, 2889, 1719, 1659, 1437, 1256, 1213, 988, 891 cm^{-1}. ^1H NMR ($CDCl_3$): δ 5.68 (m, 2H), 5.17 (s, 1H), 4.13 (t, J = 8.0 Hz, 1H), 3.59 (t, J = 8.0 Hz, 1H), 2.98 (d, J = 3.2 Hz, 1H), 2.69 (m, 1H), 2.36−2.18 (m, 3H), 1.98−1.86 (m, 2H). ^{13}C NMR ($CDCl_3$): δ 124.6, 124.5, 103.5, 72.3, 41.5, 32.9, 23.3, 23.1. HRMS (EI) m/z 140.0842 ($[M]^+$ calcd for $C_8H_{12}O_2^+$: 140.0837).

3.3.10. (1*R*,6*S*)-8-Oxabicyclo[4.3.0]non-3-en-7-one (14e). Colorless oil (75% ee). $[\alpha]^{20}_D$ −58.9 (*c* 0.30, acetone) [lit.: $[\alpha]^{20}_D$ −85.4 (*c* 2.63, acetone)].[3f] IR (neat): 3030, 2970, 2905, 2843, 1763, 1659, 1479, 1437, 1373, 1308, 1225, 1198, 1175, 1134, 1080, 1042, 1013, 995, 978, 945, 895, 800, 731, 706, 665 cm^{-1}. ^1H NMR ($CDCl_3$): δ 5.75 (d, J = 2.4 Hz, 2H), 4.32 (dd, J = 8.8, 5.1 Hz, 1H), 4.03 (dd, J = 8.8, 2.2 Hz, 1H), 2.79 (dt, J = 8.1, 2.7 Hz, 1H), 2.63 (dddd, J = 15.6, 7.3, 5.1, 2.2 Hz, 1H), 2.52 (br d, J = 17.3 Hz, 1H), 2.43−2.34 (m, 1H), 2.31−2.24

(m, 1H), 1.96−1.88 (m, 1H). ^{13}C NMR ($CDCl_3$): δ 178.6, 124.8, 124.5, 72.5, 37.2, 31.9, 24.6, 21.9. Anal. Calcd for $C_8H_{10}O_2$: C, 69.54; H, 7.30. Found: C, 69.52; H, 7.32.

3.3.11. (2*RS*,3*R,4*S**)-2-Hydroxy-3,4-diphenyltetrahydrofuran (19).** White solid (82% yield). Absolute configuration of **19** has not been determined. mp 80.5−80.6 °C. IR (neat): 3449, 3030, 2951, 2893, 1602, 1495, 1452, 1427, 1242, 1080, 1026, 980, 891, 766, 702 cm^{-1}. ^{1}H NMR ($CDCl_3$): δ 7.15−7.05 (m, 6H), 6.90 (m, 2H), 6.80 (m, 2H), 5.78 (br d, J = 2.9 Hz, 1H), 4.51 (dd, J = 8.5, 7.8 Hz, 1H), 4.24 (*t*, J = 8.5 Hz, 1H), 4.15 (ddd, J = 8.5, 7.8, 7.3 Hz, 1H), 3.55 (br d, J = 7.3 Hz, 1H), 3.07 (br d, 2.9 Hz, 1H). ^{13}C NMR ($CDCl_3$): δ 136.9, 136.8, 128.6, 128.5, 127.9, 127.7, 126.5, 126.4, 103.1, 71.5, 57.6, 47.8. HRMS (FAB) *m*/*z* 240.1148 ([M]$^+$ calcd for $C_{16}H_{16}O_2^+$: 240.1150).

3.3.12. (3*R,4*S**)-3,4-Diphenyldihydrofuran-2-one (20).** White solid (81% ee). Absolute configuration of **20** has not been determined. $[\alpha]^{24}_D$ −121.7 (*c* 0.20, $CHCl_3$). mp 126.6−126.7 °C. IR (KBr): 3063, 3028, 1763, 1497, 1477, 1452, 1379, 1364, 1215, 1169, 1150, 1082, 1022, 968, 953, 918, 853, 758, 735, 714, 698, 644 cm^{-1}. ^{1}H NMR ($CDCl_3$): δ 7.12 (m, 6H), 6.83 (m, 4H), 4.72 (m, 2H), 4.25 (d, J = 8.5 Hz, 1H), 4.00 (ddd, J = 8.5, 6.1, 4.4 Hz, 1H). ^{13}C NMR ($CDCl_3$): δ 176.2, 136.5, 129.2, 128.3, 128.0, 127.8, 127.3, 127.2, 71.3, 52.1, 47.8. Anal. Calcd for $C_{16}H_{14}O_2 \cdot {}^1/_8H_2O$: C, 79.89; H, 5.97. Found: C, 79.91; H, 5.92. HRMS (FAB) *m*/*z* 239.1078 ([M + H]$^+$ calcd for $C_{16}H_{15}O_2^+$: 239.1072).

3.3.13. (2*RS*,3*R,4*S**)-3,4-Dicyclohexyl-2-hydroxytetrahydrofuran (21).** White solid (82% yield), a single diastereomer. Absolute configuration of **21** has not been determined. mp 126.4−126.5 °C. IR (KBr): 3356, 2853, 2665, 1447, 1350, 1277, 1148, 1115, 1055, 1026, 988, 905, 783, 762, 718, 633 cm^{-1}. ^{1}H NMR ($CDCl_3$): δ 5.34 (dd, J = 3.2, 2.0 Hz, 1H), 4.07 (t, J = 8.1 Hz, 1H), 3.68 (t, J = 8.1 Hz, 1H), 2.78 (d, J = 3.2 Hz, −OH), 2.31 (quint., J = 8.1 Hz, 1H), 1.92 (m, 1H), 1.79−1.60 (m, 9H), 1.50−0.98 (m, 13H). ^{13}C NMR ($CDCl_3$): δ 101.0, 71.4, 53.4, 46.0, 36.2, 35.1, 33.6, 33.1, 31.7, 30.0, 26.9, 26.6, 26.5, 26.45, 26.40, 26.3. Anal. Calcd for $C_{16}H_{28}O_2$: C, 76.14; H, 11.18. Found: C, 75.86; H, 11.19.

3.3.14. (2*RS*,3*R,4*S**)-2-Benzyloxy-3,4-dicyclohexyltetrahydrofuran (22).** To a solution of **21** (8.4 mg, 33 μmol) in CH_2Cl_2 were added benzyl alcohol (18 μL, 5 equiv) and (*RS*)-10-camphorsulfonic acid (2.3 mg, 0.3 equiv). After being stirred for 1 h, the resulting mixture was directly purified by silica gel column chromatography (*n*-hexane/ethyl acetate = 9/1) to give a 7:1 diastereomeric mixture of **22** (10.2 mg, 90%) as a colorless oil. IR (neat): 3063, 3030, 2849, 2665, 1946, 1871, 1807, 1605, 1495, 1448, 1354, 1308, 1265, 1225, 1150, 976, 923, 891, 735, 698 cm^{-1}. ^{1}H NMR of the major isomer ($CDCl_3$): δ 7.34−7.24 (m, 5H), 5.00 (d, J = 1.7 Hz, 1H), 4.71 (d, J = 12 Hz, 1H), 4.46 (d, J = 12 Hz, 1H), 4.00 (t, J = 8.1 Hz, 1H), 3.69 (t, J = 8.1 Hz, 1H), 2.28 (quint., J = 8.1 Hz, 1H), 2.02 (m, 1H), 1.77−0.85 (m, 22H). ^{1}H NMR of the minor isomer ($CDCl_3$): δ 7.34−7.24 (m, 5H), 4.94 (br s, 1H), 4.69 (d, J = 12 Hz, 1H), 4.44 (d, J = 12 Hz, 1H), 3.97 (t, J = 8.1 Hz, 1H), 3.67 (m, 1H), 1.90 (m, 1H), 1.79 (m, 1H), 1.75−0.80 (m, 22H). ^{13}C NMR of the major isomer ($CDCl_3$): δ 138.2, 128.0, 127.4, 127.0, 105.8, 71.1, 68.8, 52.3, 46.0, 36.2, 35.0, 33.4, 33.0, 31.5, 29.9, 26.7, 26.44, 26.39, 26.28, 26.26, 26.2. ^{13}C NMR of the minor isomer ($CDCl_3$): δ 138.2, 127.9, 127.3, 127.0, 105.6, 70.3, 68.2, 54.5, 46.9, 41.5, 40.6, 32.6, 31.8, 31.3, 29.4, 26.6, 26.5. The chemical shifts (26.7, 26.44, 26.39, 26.28, 26.26, and 26.2) of six carbons were identical to those of the corresponding carbons of the major isomer. Anal. Calcd for $C_{23}H_{34}O_2$: C, 80.65; H, 10.01. Found for the diastereomeric mixture: C, 80.35; H, 9.87.

3.3.15. (1*S,2*S**,5*R**,6*R**,7*RS*)-7-Hydroxy-8-oxa-2,5-diphenylbicyclo[4.3.0]nonane (24a).** White solid (98% yield). mp 146.9−147.0 °C. IR (KBr): 3369, 2937, 2874, 1597, 1493, 1448, 1367, 1331, 1219, 1084, 1007, 907, 770, 729, 694 cm^{-1}. ^{1}H NMR ($CDCl_3$): δ 7.35−7.20 (m, 10H), 5.23 (br s, 1H), 3.96 (t, J = 9.3 Hz, 1H), 3.89 (dd, J = 9.3, 3.7 Hz, 1H), 3.41 (m, 2H), 3.06 (m, 1H), 2.85 (dt, J = 9.5, 5.1 Hz, 1H), 2.21−1.98 (m, 5H). ^{13}C NMR ($CDCl_3$): δ 144.1, 143.5, 128.34(2), 128.32(2), 127.4(4), 126.1, 126.0, 100.4, 68.3, 51.1, 41.9, 37.3, 36.5, 21.9, 21.8 (the number in parentheses means the number of overlapping carbon signals). Anal. Calcd for $C_{20}H_{22}O_2$: C, 81.60; H, 7.53. Found: C, 81.44; H, 7.54.

3.3.16. (1*S,2*S**,5*R**,6*R**)-8-Oxa-2,5-diphenylbicyclo[4.3.0]nonan-7-one (25a).** White solid (93% ee). $[\alpha]^{24}_D$ −71.3 (*c* 0.31, $CHCl_3$). mp 164.4−164.5 °C. IR (KBr): 3028, 2916, 2874, 1763, 1495, 1375, 1167, 1121, 1026, 772, 750, 700 cm^{-1}. ^{1}H NMR ($CDCl_3$): δ 7.43 (m, 2H), 7.35 (m, 4H), 7.26 (m, 4H), 4.06 (dd, J = 10, 3.9 Hz, 1H), 3.98 (dd, J = 10, 7.8 Hz, 1H), 3.54 (m, 1H), 3.44 (m, 1H), 3.22 (m, 2H), 2.29 (m, 1H), 2.10 (m, 3H). ^{13}C NMR ($CDCl_3$): δ 177.0, 141.6, 141.1, 128.6-(2), 128.1(2), 128.0(2), 127.4(2), 126.7, 126.6, 67.5, 44.0, 40.6, 37.9, 37.0, 23.9, 22.0. HRMS (FAB) *m*/*z* 293.1539 ([M + H]$^+$ calcd for $C_{20}H_{21}O_2^+$: 293.1542).

3.3.17. (1*S,2*S**,5*R**,6*R**,7*RS*)-7-Hydroxy-8-oxa-2,5-diphenylbicyclo[4.3.0]non-3-ene (24b).** White solid (98% yield). mp 83.3−83.9 °C. IR (KBr): 3479, 3022, 2961, 2893, 2853, 1599, 1489, 1450, 1429, 1269, 1236, 1078, 1011, 982, 752, 706 cm^{-1}. ^{1}H NMR ($CDCl_3$): δ 7.39−7.25 (m, 10H), 6.31 (m, 2H), 4.96 (m, 1H), 3.72−3.66 (m, 3H), 3.58 (dd, J = 9.0, 6.1 Hz, 1H), 3.19 (m, 1H), 2.91 (br t, J = 7.6 Hz, 1H), 2.09 (br d, J = 3.2 Hz, 1H). ^{13}C NMR ($CDCl_3$): δ 142.1, 141.5, 130.9, 130.8, 128.31(2), 128.25(2), 128.21(2), 127.7(2), 126.3, 126.2, 101.0, 69.3, 51.2, 43.1, 41.2, 40.4. HRMS (FAB) *m*/*z* 292.1469 ([M]$^+$ calcd for $C_{20}H_{20}O_2^+$: 292.1463).

3.3.18. (1*S,2*S**,5*R**,6*R**)-8-Oxa-2,5-diphenylbicyclo[4.3.0]non-3-en-7-one (25b).** White solid (90% ee). $[\alpha]^{23}_D$ −124.6 (*c* 0.10, $CHCl_3$). mp 116.7−116.8 °C. IR (KBr): 3059, 3030, 2972, 2910, 2826, 1962, 1892, 1763, 1599, 1495, 1450, 1379, 1302, 1271, 1232, 1167, 1119, 1072, 1047, 1016, 988, 908, 783, 739, 698 cm^{-1}. ^{1}H NMR ($CDCl_3$): δ 7.41−7.28 (m, 10H), 6.28 (br s, 2H), 3.89 (m, 2H), 3.85 (d, J = 9.0 Hz, 1H), 3.57 (dd, J = 9.0, 7.8 Hz, 1H), 3.31 (br t, J = 9.0 Hz, 1H), 3.22 (m, 1H). ^{13}C NMR ($CDCl_3$): δ 176.6, 140.3, 139.5, 130.7, 129.2-(2), 129.0, 128.8(2), 128.3(2), 127.6(2), 127.3, 127.0, 69.1, 43.7, 40.1, 39.3, 38.8. HRMS (FAB) *m*/*z* 291.1380 ([M + H]$^+$ calcd for $C_{20}H_{19}O_2^+$: 291.1385).

3.4. Syntheses of *meso*-Diols 15 and 16. 3.4.1. *meso*-2,3-Diphenylbutane-1,4-diol (15). A suspension of platinum(IV) oxide (50 mg, 0.22 mmol) and diphenylmaleic anhydride in anhydrous ethanol/CH_2Cl_2 (5.0 mL/5.0 mL) was placed in a 50 mL round-bottom flask under H_2 at 1 atm. After being vigorously stirred for 1day at room temperature, the reaction mixture was filtered through a pad of Celite and evaporated. The residue was used without further purification in the following experiment. To a solution of the crude product (ca. 200 mg) in THF (5.0 mL)) was slowly added lithium aluminum hydride (LAH) in THF solution (1 M, 2.0 mL, 2.0 mmol) at 0 °C. After being stirred for 1 day, the reaction mixture was quenched with aqueous 3% NaOH (1.0 mL). The resulting suspension was filtered through a pad of Celite, and the filtrate was evaporated under reduced pressure and submitted to flash column chromatography (*n*-hexane/ethyl acetate = 1/1) to give *meso*-diol **15** (96 mg, 40%) and DL-diol (52 mg, 22%).[53] *meso*-2,3-Diphenylbutane-1,4-diol (**15**) was obtained as a white solid. mp 144.0−144.1 °C. IR (KBr): 3445, 2961, 2889, 1601, 1495, 1454, 1373, 1217, 1184, 1082, 1051, 974, 758, 702 cm^{-1}. ^{1}H NMR ($CDCl_3$): δ 7.35 (m, 10H), 3.56 (m, 4H), 3.12 (m, 2H), 1.12 (dd, J = 7.8, 5.1 Hz, 2H). ^{13}C NMR ($CDCl_3$): δ 140.3, 128.7(2), 128.1(2), 127.0, 65.5, 50.6. HRMS (FAB) *m*/*z* 243.1390 ([M + H]$^+$ calcd for $C_{16}H_{19}O_2^+$: 243.1385).

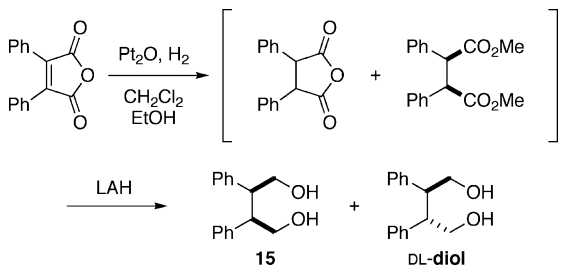

3.4.2. *meso*-2,3-Dicyclohexylbutane-1,4-diol (16). To a solution of *meso*-2,3-diphenylbutane-1,4-diol (**15**, 135 mg, 0.56 mmol) in ethanol (2.0 mL) was added rhodium on alumina (5 wt %, 270 mg). The mixture was vigorously stirred at 120 °C under 90 bar of hydrogen. After the hydrogen uptake ceased (ca. 4 days), the slushy mixture was filtered through a pad of Celite and evaporated under reduced pressure. Purification of the residue by silica gel column chromatography (CH_2Cl_2/acetone = 4/1) gave *meso*-diol **16** (100 mg, 70%) as a white solid. mp 128.2−128.3 °C. IR (KBr): 3287, 2918, 2849, 1485, 1445, 1331, 1234, 1030, 989, 889, 2961 cm^{-1}. ^1H NMR ($CDCl_3$): δ 3.79 (dd, J = 10.7, 6.6 Hz, 2H), 3.63 (dd, J = 10.7, 3.4 Hz, 2H), 2.53 (s, 2H, −OH), 1.82−1.56 (m, 12H), 1.45 (m, 2H), 1.30−0.97 (m, 10H). ^{13}C NMR ($CDCl_3$): δ 63.0, 47.6, 38.2, 33.3, 31.2, 27.0, 26.9, 26.7. Anal. Calcd for $C_{16}H_{30}O_2$: C, 75.54; H, 11.89. Found: C, 75.29; H, 11.82.

3.5. Syntheses of *meso*-Diols 23a and 23b. 3.5.1. (1*R,2*S**,3*S**,6*R**)-1,2-Bis(hydroxymethyl)-3,6-diphenylcyclohexane (23a).** In a 200 mL round-bottom flask were placed (1*R**,2*S**,3*S**,6*R**)-3,6-diphenyl-1,2,3,6-tetrahydrophthalic anhydride (**54**, 2.0 g, 6.6 mmol), Pd/C (5% Pd on active charcoal, 300 mg), and CH_2Cl_2 (30 mL). The flask was purged with H_2 and installed with a rubber balloon filled with H_2. After being stirred overnight at room temperature, the mixture was filtered through a pad of Celite and evaporated to afford a crude hydrogenated product in a quantitative yield. The crude product was used for the next reaction without further purification. To a solution of the crude product in THF (50 mL) was carefully added a THF solution of LAH (1 M, 13 mL, 2.0 eq) at 0 °C, and, after being stirred for 1 day, the reaction mixture was quenched with aqueous 2% NaOH (2.0 mL). The resulting suspension was filtered through a pad of Celite, and the filtrate was evaporated under reduce pressure. Purification of the crude product by silica gel column chromatography (CH_2Cl_2/acetone = 4/1) gave *meso*-diol **23a** (987 mg, 51%) as a white solid. mp 132.3−132.4 °C. IR (KBr): 3429, 3315, 2924, 2864, 1601, 1495, 1450, 1371, 1078, 1015, 758, 702 cm^{-1}. ^1H NMR ($CDCl_3$): δ 7.38−7.18 (m, 10H), 3.58 (dd, J = 11.2, 5.4 Hz, 2H), 3.50 (dd, J = 11.2, 7.1 Hz, 2H), 3.15 (m, 2H), 2.40 (m, 4H), 2.02 (m, 2H), 1.62 (s, 2H). ^{13}C NMR ($CDCl_3$): δ 143.9, 128.2(2), 127.9, 126.2(2), 62.2, 46.2, 41.9, 27.5. HRMS (FAB) m/z 297.1848 ([M + H]$^+$ calcd for $C_{20}H_{25}O_2^+$: 297.1855).

3.5.2. (1*R,2*S**,3*S**,6*R**)-1,2-Bis(hydroxymethyl)-3,6-diphenylcyclohex-4-ene (23b).** To a solution of anhydride **54** (2.0 g, 6.6 mmol) in ether (50 mL) was carefully added a solution of diisobutyl aluminum hydride in *n*-hexane (0.95 M, 35 mL, 5.0 equiv) at 0 °C, and, after being stirred for 6 h, the reaction mixture was quenched with aqueous HCl (2 M, 20 mL). The whole mixture was extracted with ethyl acetate (50 mL × 3), and the combined organic layers were washed with brine, dried over $MgSO_4$, filtered, and evaporated. Purification of the residue by silica gel column chromatography (CH_2Cl_2/acetone = 4/1) gave **23b** (1.6 g, 83%) as a white solid. mp 96.8−97.0 °C. IR (KBr): 3260, 3022, 2934, 2874, 1599, 1491, 1450, 1385, 1011, 920, 858, 748, 704 cm^{-1}. ^1H NMR ($CDCl_3$): δ 7.44−7.22 (m, 10H), 6.12 (s, 2H), 3.84 (d, J = 6.3 Hz, 2H), 3.60 (dd, J = 11.5, 6.8 Hz, 2H), 3.36 (dd, J = 11.5, 5.6 Hz, 2H), 2.53 (m, 2H). ^{13}C NMR ($CDCl_3$): δ 141.2, 130.3, 128.6(2), 128.2(2), 126.5, 62.0, 43.8, 43.1. HRMS (FAB) m/z 295.1691 ([M + H$^+$] calcd for $C_{20}H_{23}O_2^+$: 295.1698).

3.6. Oxidation of *exo*-Bicyclo[6.1.0]nonan-9-ol. *exo*-Bicyclo[6.1.0]-nonan-9-ol (**27**) was prepared by hydroboration of 9,9-dibromobicyclo-[6.1.0]nonane according to the previously reported method with slight modification.[37] Compound **27** (14.0 mg, 0.1 mmol) and complex **4** (2.0 mg, 2.0 mol %) were dissolved in anhydrous $CHCl_3$ (0.5 mL). The solution was stirred under irradiation with a halogen lamp in air for 12 h at 0 °C. A half part of the mixture was directly submitted to silica gel chromatography (*n*-hexane/ethyl acetate = 19/1 to 4/1) to give a cis and trans mixture of 10,11-dioxabicyclo[6.3.0]undecan-9-ol (**28**, 4.9 mg, 56%) as a colorless oil. Because the isolated **28** was unstable at room temperature, it was stored at −30 °C. To determine the relative configuration of the isomers, the remaining half mixture was submitted to LAH reduction. A THF solution of LAH (1.0 M, 50 μL) was added dropwise to the reaction mixture at 0 °C under nitrogen atmosphere. The solution was allowed to stir at 0 °C for 2 h. The reaction mixture was quenched by water (0.5 mL), acidified with 10% H_2SO_4, and extracted with EtOAc (5 mL × 3). The combined organic phase was washed with aqueous $NaHCO_3$ and brine, dried over $MgSO_4$, filtered, and evaporated. Purification of the residue by silica gel column chromatography (*n*-hexane/ethyl acetate = 9/1 to 3/7) afforded a 32:68 mixture of *cis*- and *trans*-2-(hydroxymethyl)cyclooctanols (**29**, 3.5 mg, 44%) as colorless oil. The relative configuration of each isomer was assigned by comparing its NMR data to those of the reported one.[38]

***exo*-Bicyclo[6.1.0]nonan-9-ol[37b] (27).** Colorless crystals. mp 30.9−31.0 °C. IR ($CHCl_3$): 3601, 3446, 1101 cm^{-1}. ^1H NMR ($CDCl_3$): δ 2.87 (t, J = 2.2 Hz, 1H), 2.26 (br s, 1H, −OH), 2.04 (m, 2H), 1.65 (m, 2H), 1.51 (m, 2H), 1.31 (m, 4H), 0.87 (m, 4H). ^{13}C NMR ($CDCl_3$): δ 56.8, 29.1, 26.5, 25.3, 24.8. Anal. Calcd for $C_9H_{16}O$: C, 77.09; H, 11.50. Found: C, 76.81; H, 11.46.

10,11-Dioxabicyclo[6.3.0]undecan-9-ol (28). Colorless oil. IR ($CHCl_3$): 3587, 3501, 3024, 2930, 2856, 1049 cm^{-1}. ^1H NMR of *trans*-isomer (C_6D_6): δ 4.90 (d, J = 1.7 Hz, 1H), 3.97 (ddd, J = 10.0, 8.1, 4.2 Hz, 1H), 2.87 (br s, 1H, OH), 2.49 (dddd, J = 12.5, 8.1, 4.2, 1.7 Hz, 1H), 1.79 (m, 1H), 1.62 (m, 1H), 1.46−1.29 (m, 5H), 1.22−0.88 (m, 5H). ^1H NMR of *cis*-isomer (C_6D_6): δ 5.06 (d, J = 4.6 Hz, 1H), 4.08 (ddd, J = 9.5, 8.3, 3.9 Hz, 1H), 2.71 (br s, 1H, OH), 2.20 (ddt, J = 10.3, 8.4, 4.6 Hz, 1H), 1.89 (m, 1H), 1.52 (m, 1H), 1.46−1.29 (m, 5H), 1.22−0.88 (m, 5H). ^{13}C NMR of *trans*-isomer (C_6D_6): δ 106.2, 86.6, 61.5, 31.5, 30.3, 27.5, 26.9, 24.7, 23.7. ^{13}C NMR of *cis*-isomer (C_6D_6): δ 100.0, 82.7, 58.1, 33.2, 28.0, 27.4, 26.94, 26.0, 23.5. Anal. Calcd for $C_9H_{16}O_3$: C, 62.77; H, 9.36. Found: C, 62.50; H, 9.37.

2-(Hydroxymethyl)cyclooctanol[38] (29). Colorless oil. IR ($CHCl_3$): 3614, 3447, 3007, 2928, 2858 cm^{-1}. ^1H NMR of *trans*-isomer ($CDCl_3$): δ 3.81 (ddd, J = 9.4, 6.2, 2.7 Hz, 1H), 3.74−3.63 (m, 2H), 3.00 (br s, 1H, −OH), 2.95 (br s, 1H, −OH), 1.89−1.29 (m, 13H). ^1H NMR of *cis*-isomer ($CDCl_3$): δ 4.10 (ddd, J = 8.7, 5.4, 2.7 Hz, 1H), 3.74−3.63 (m, 2H), 2.52 (br s, 1H, −OH), 2.29 (br s, 1H, −OH), 1.89−1.29 (m, 13H). ^{13}C NMR of *trans*-isomer ($CDCl_3$): δ 77.6, 69.7, 44.3, 34.0, 27.2, 26.8, 26.5, 25.4, 22.9. ^{13}C NMR of *cis*-isomer ($CDCl_3$): δ 73.3, 67.8, 41.8, 32.8, 27.5, 27.4, 25.5, 23.8, 22.2.

(a*S*)-3-Formyl-2-hydroxy-2′-(4-biphenylyl)-1,1′-binaphthyl (53). Compound **53** was prepared in a manner similar to the reported procedure.[12] Yellow crystals. mp 275.6−275.9 °C. $[\alpha]^{23}_D$ +94.6 (*c* 0.60, $CHCl_3$). IR (KBr): 3209, 3026, 2851, 1655, 1340, 1290, 1180, 1117, 939, 895, 758 cm^{-1}. ^1H NMR ($CDCl_3$): δ 10.44 (s, 1H), 10.09 (s, 1H), 8.17 (s, 1H), 8.06 (d, J = 8.5 Hz, 1H), 7.98 (d, J = 8.1 Hz, 1H), 7.85 (d, J = 8.3 Hz, 1H), 7.69 (d, J = 8.5 Hz, 1H), 7.46 (m, 3H), 7.36−7.24 (m, 11H), 7.15 (d, J = 8.3 Hz, 1H). ^{13}C NMR ($CDCl_3$): δ 196.4, 153.3, 140.7, 140.4, 140.1, 138.8, 137.8, 137.7, 132.8, 132.5, 130.2, 129.7, 129.5, 128.9, 128.5, 128.4, 128.1, 127.0, 126.9, 126.7, 126.5, 125.9, 125.7, 125.2, 124.1, 121.4, 121.1 (27 signals were observed, because six signals overlapped with other signals). HRMS (FAB) m/z 450.1623 ([M$^+$] calcd for $C_{33}H_{22}O_2^+$: 450.1620).

3.7. Measurement of Kinetic Isotope Effect (Scheme 3). Determination of Intermolecular Kinetic Isotope Effect of the Oxidation of 12a. The oxidation reactions of **12a** and **12a**-d_4 using complex **4** as the catalyst were performed at room temperature in a manner similar to that described for the oxidation of **12a** except for the presence of 2-bromonaphtharene as the internal standard. An aliquot of the mixture was taken out before starting irradiation and subjected to ^1H NMR analysis to give T_0 NMR data. The reactions were monitored by ^1H NMR measurement at intervals of ca. 3 h (for oxidation with **5**) and of ca. 15 min (for oxidation with **4**) until the conversion amounted to 10%. The absorption of methine protons at C1 and C2 of **12a** and **12a**-d_4 was used as diagnostic signals for monitoring the reaction by ^1H

(53) *meso*-2,3-Diphenylbutane-1,4-diols (**15**) and its DL-isomer were identified by HPLC analysis using DAICEL CHIRALCEL OD-H (*n*-hexane/*i*-PrOH = 90/10, flow rate 0.5 mL/min), respectively: the former gave a single peak, while the latter gave two peaks.

NMR analysis. The relative reaction rate was determined by the slopes of the plots ($-\ln[S]/[S_0]$ vs reaction time for the oxidation with **4**; conversion vs reaction time for the oxidation with **5**). Every measurement was repeated at least three times. The average value and standard error were calculated on the data and are shown in Table 5.

Determination of Intermolecular Kinetic Isotope Effect of the Oxidation of 26 under Independent Measurement Conditions. The KIE measurement for the oxidation of **26** and **26**-d_2 using **4** or **5** as catalyst was carried out in a manner similar to that described for the oxidation of **12a** and **12a**-d_4. The absorption of methylene protons at C2 and C3 of **26** and **26**-d_2 was used as diagnostic signals.

Determination of Intermolecular Kinetic Isotope Effect of the Oxidation of 26 under Competition Conditions. A 1:1 mixture of **26** and **26**-d_2 (0.05 mmol each), pentamethylbenzene (14.8 mg, 0.1 mmol) as the internal standard, and catalyst (**4** or **5**, 2 μmol) were dissolved in benzene-d_6 (1 mL). The oxidation was carried out in the same manner as the oxidation of **12a**. When 10% of the starting materials (**26** and **26**-d_2) was consumed (1 h for the oxidation with **4** and 12 h for the oxidation with **5**), the reaction mixture was filtered through a short silica gel column. The H/D relative reaction ratio and conversion of starting material were determined by ^{1}H NMR analysis, on the basis of the integration ratio of the proton signals at C1 and C2 of the unreacted alcohol. Every measurement was repeated at least three times. The average value and standard error were calculated on the data and are shown in Table 5.

Determination of Intramolecular Kinetic Isotope Effect of the Oxidation of 26. Compound **26**-d_1 (13.7 mg, 0.1 mmol), pentamethylbenzene (14.8 mg, 0.1 mmol) as the internal standard, and catalyst (**4** or **5**, 2 μmol) were dissolved in benzene-d_6 (1 mL). The oxidation was carried out under the same conditions as the oxidation of **12a**. The H/D relative reaction ratio was determined by ^{1}H NMR analysis, on the basis of the integration ratio of the proton signals at C1 and C3 of the resulting aldehyde. Every measurement was repeated at least three times. The average value and standard error were calculated on the data and are shown in Table 5.

3.8. Study of Photolysis of 4 and 5 by UV/Visible Analysis. Photolysis of complex **4** and **5**: Each of the catalysts **4** and **5** was dissolved in benzene in a concentration of 2.0×10^{-5} mol L^{-1}, and the solution (2 mL) was placed in a quartz cell with 1 cm path length. The solution was stirred at room temperature under irradiation with a halogen lamp (150 W) in air. The photolysis was monitored by consecutive measurement of UV/visible spectra.

Photolysis of complex **4** and **5** in the presence of **12a**: Each of the catalysts **4** and **5** was dissolved in benzene in a concentration of 2.0×10^{-5} mol L^{-1}. To this solution was added diol **12a** (57.7 mg, 0.4 mmol), and the mixture was placed in a quartz cell with 1 cm path length. The solution was stirred at room temperature under irradiation with a halogen lamp (150 W) in air. The photolysis was monitored by consecutive measurement of UV/visible spectra.

3.9. Study of Dependence of Oxidation Rates on Oxygen Concentration. Diol **12a** (14.4 mg, 0.1 mmol), pentamethylbenzene (14.8 mg, 0.1 mmol) as the internal standard, and catalyst (**4** or **5**, 2 μmol) were dissolved in benzene-d_6 (1 mL). The oxidation reactions were performed under the standard conditions, according to a recently reported balloon technique[20] using a balloon that was filled with different ratios of oxygen to nitrogen. The ratio of oxygen to nitrogen was established by measuring the flow rate of each gas with a KOFLOC RK-1650 gas flow meter. The balloon was filled to just about the same pressure (1atm) for each trial. The reaction was monitored by ^{1}H NMR measurement until the conversion amounted to 10%. In the case of the oxidation with **4**, the reaction rates were determined by plotting $-\ln[S]/[S_0]$ against reaction time, while the reaction rates for the oxidation with **5** were established by plotting conversion of **12a** against reaction time. The reaction rates were plotted against the % oxygen. The order of the reaction with respect to oxygen concentration was calculated by plotting log k against log[O_2] for each catalyst. The order of the reaction of **26** with respect to oxygen concentration was also determined by the same procedure.

Acknowledgment. We thank Professor Keisuke Suzuki, Tokyo Institute of Technology, and Professor Shunichi Fukuzumi, Osaka University, for helpful discussions and the reviewers for their constructive criticism of the present study.

JA047608I